minerals

MDPI

Review

Complexation of REE in Hydrothermal Fluids and Its Significance on REE Mineralization

Jian Di [1,2,3] and Xing Ding [1,2,3,*]

[1] State Key Laboratory of Isotope Geochemistry, Guangzhou Institute of Geochemistry, Chinese Academy of Sciences, Guangzhou 510640, China; dijian@gig.ac.cn
[2] CAS Center for Excellence in Deep Earth Science, Guangzhou Institute of Geochemistry, Guangzhou 510640, China
[3] University of Chinese Academy of Sciences, Beijing 100101, China
* Correspondence: xding@gig.ac.cn

Abstract: Rare earth elements (REEs) have recently been classified as critical and strategic metals due to their importance in modern society. Research on the geochemical behaviors and mineralization of REEs not only provides essential guidance for mineral exploration but also holds great significance in enhancing our understanding of Earth's origin and evolution. This paper reviews recent research on the occurrence characteristics, deposit types, and hydrothermal behaviors of REEs, with a particular focus on comparing the complexation and transport of REEs by F, Cl, S, C, P, OH, and organic ligands in fluids. Due to the very weak hydrolysis of REE ions, they predominantly exist as either hydrated ions or free ions in low-temperature and acidic to weakly basic fluids. As the ligand activity increases, the general order of transporting REEs is $Cl^- \approx SO_4^{2-} > F^- \approx PO_4^{3-} > CO_3^{2-} > OH^-$ under acidic conditions or $OH^- > SO_4^{2-} \approx Cl^- > F^-$ under alkaline conditions. In acidic to neutral hydrothermal systems, the transport of REEs is primarily dominated by SO_4^{2-} and Cl^- ions while the deposition of REEs could be influenced by F^-, CO_3^{2-}, and PO_4^{3-} ions. In neutral to alkaline hydrothermal systems, REEs mainly exist in fluids as hydroxyl complexes or other ligand-bearing hydroxyl complexes. Additionally suggested are further comprehensive investigations that will fill significant gaps in our understanding of mechanisms governing the transport and enrichment of REEs in hydrothermal fluids.

Keywords: rare earth elements; REE; complexation; speciation; REE complex; hydrothermal fluids

check for updates

Citation: Di, J.; Ding, X. Complexation of REE in Hydrothermal Fluids and Its Significance on REE Mineralization. *Minerals* **2024**, *14*, 531. https://doi.org/10.3390/min14060531

Academic Editor: Pierpaolo Zuddas

Received: 16 April 2024
Revised: 11 May 2024
Accepted: 15 May 2024
Published: 21 May 2024

Copyright: © 2024 by the authors. Licensee MDPI, Basel, Switzerland. This article is an open access article distributed under the terms and conditions of the Creative Commons Attribution (CC BY) license (https://creativecommons.org/licenses/by/4.0/).

1. Introduction

Rare earth elements (REEs) are located in Group IIIB of the periodic table and consist of lanthanide, Sc (atomic number 39), and Y (atomic number 21) [1,2]. This series of elements can form stable +3 valence cations with similar ionic radii, resulting in similar physical and chemical properties and consistent geochemical behaviors during most geological activities [3–5].

In the modern world, REEs play an indispensable role in emerging technologies, green industries, and cutting-edge applications such as chemical catalysts, alloys, glass-polishing, aerospace technologies, permanent magnets, green energy production, national defense, and security [6–8]. These unique physical and chemical properties have earned them the moniker "The Vitamins of Modern Industry" [9–16]. Given their critical supply risk, irreplaceability, and substantial economic significance in modern technology sectors, worldwide recognition has led to REEs being included in the "Critical (Strategic) Raw Materials/Metals" catalogs by many countries for resource control purposes [17–22]. Consequently, research on the fundamental properties, mineralization, and mining applications of REEs has become a prominent topic [8,23–29].

Studying the fundamental properties of REEs is crucial not only for deciphering the evolution of Earth but also for providing theoretical insights into regional mineral exploration. Currently, evidence of fluid activity has been discovered in numerous rare earth and rare metal deposits [30–33]. Experimental studies further confirm that REEs could form stable complexes with various ligands in fluids (e.g., F^-, Cl^-, SO_4^{2-}, CO_3^{2-}, PO_4^{3-} and OH^-) and thus have the potential to be transported in the form of these complexes ([34] and references therein). In this paper, we provide a summary of recent experimental geochemical, geological, and thermodynamic research on REEs in different hydrothermal systems. This synthesis aims to offer theoretical insights into the hydrothermal geochemical behaviors of REEs during magma differentiation, hydrothermal alteration, and rock weathering to promote an understanding of REE mineralization.

2. Geochemical Character of REEs

REEs comprise a group of 17 elements, namely, La, Ce, Pr, Nd, Pm*, Sm, Eu, Gd, Tb, Dy, Ho, Er, Tm, Yb, Y, and Sc [2]. The geochemical behavior of REEs is quite similar, as they typically occur together in minerals with varying concentrations. Their comparable physical and chemical properties also pose challenges to the separation and purification processes of REEs [35]. Pm* stands out among the REEs due to its radioactive nature and lack of stable isotopes and has vanishingly small content in the crust [6,9,11,35]. Additionally, Sc shares many properties with REEs but is rarely coexistent with REEs in minerals. Moreover, Sc does not selectively combine with common ore-forming anions [36].

The abundance of different REEs in the crust exhibits significant variation. Generally, their abundance decreases with increases in their atomic number, as per the Oddo–Harkins rule which suggests that elements with even atomic numbers are more abundant than those with odd atomic numbers. Therefore, Ce stands out as the most abundant REE in the crust (Table 1), while Lu is particularly rare [8]. The ratio of light rare earth oxides to heavy rare earth oxides (LREO/HREO) in the crust is approximately 13:1 [11]. REEs in the crust are not low, with an average value of 63 ppm for Ce and 31 ppm for La, surpassing the average abundances of copper (28 ppm) and lead (17 ppm). Furthermore, Lu has an average crustal abundance of 0.31 ppm, much lower than that of most important metals but still higher than gold, silver, and platinum-group elements [37].

Table 1. Classification of REEs and average crustal abundances [1].

Element	Atomic Number	IPUAC Classification	Average Crust (ppm) [2]
La	57	Light	31
Ce	58	Light	63
Pr	59	Light	7.1
Nd	60	Light	27
Pm	61	Light	-
Sm	62	Light	4.7
Eu	63	Light	1
Gd	64	Light	4
Tb	65	Heavy	0.7
Dy	66	Heavy	3.9
Ho	67	Heavy	0.83
Er	68	Heavy	2.3

Table 1. *Cont.*

Element	Atomic Number	IPUAC Classification	Average Crust (ppm) [2]
Tm	69	Heavy	0.3
Yb	70	Heavy	2
Lu	71	Heavy	0.31
Y	39	Heavy	39
Sc	21	None	14

- = Concentration too low to assess as a result of the short radioactive half-life of Pm. [1] Adapted from [11] and [38]; [2] According to [37].

Under specific conditions, some REEs can exhibit noticeable composition variations, such as significant negative anomalies observed in Eu and Ce under reduced and oxidized conditions, respectively [39–43], as well as REE fractionation driven by thermal diffusion [44–46]. REEs typically occur as trivalent cations. However, certain elements may also display alternative valent states; for instance, Eu and Yb can exist in a +2 valent state while Ce and Tb can occur in a +4 valent state (Figure 1). As the atomic number increases within the lanthanide series, there is a decrease in the ionic radii of REE ions due to what is known as "lanthanide contraction" [3,47]. This trend arises from the increased attraction between the nuclei of lanthanide elements and their respective 6s electrons. The enhanced attraction is not counterbalanced by additional electrons due to poor shielding properties exhibited by the 4f electrons [2,48].

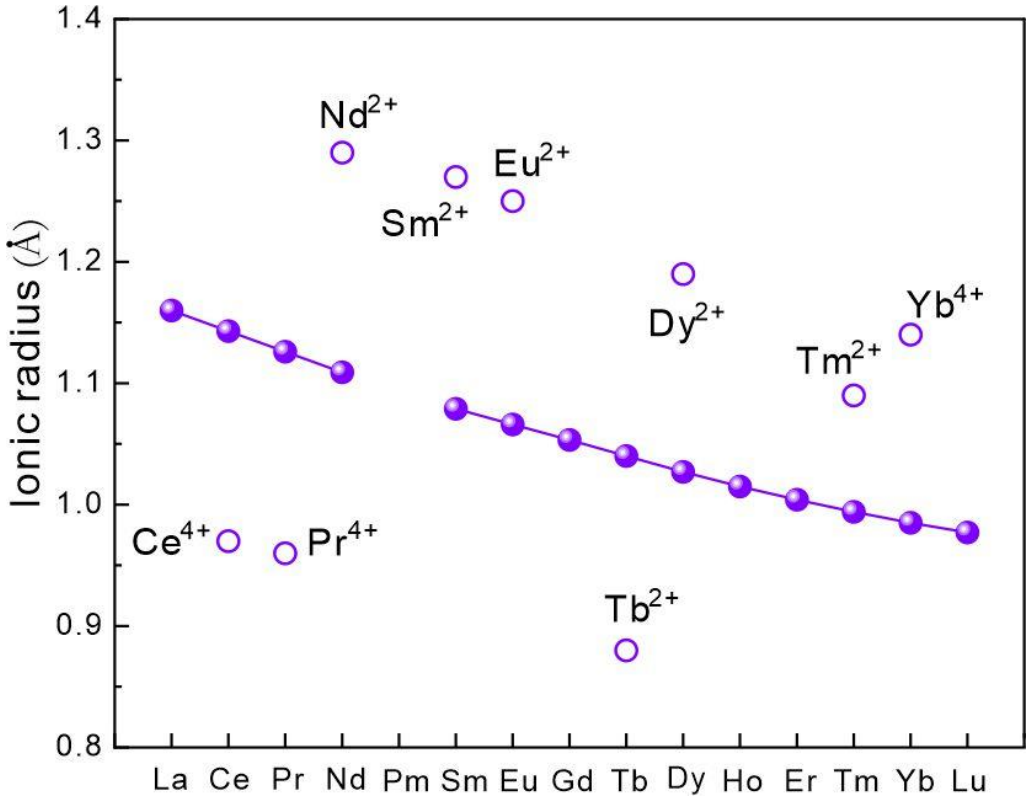

Figure 1. The ionic radius of REEs in VII coordination. The radius values are from Henderson (1984) [3].

3. Occurrence of REEs

Typically, REEs exhibit a high coordination number in minerals. For example, light REEs are commonly found in carbonates and phosphates with 8 to 10 coordination, while

heavy REEs are predominantly present as oxides or phosphate minerals with 6 to 8 coordination. Both LREEs and HREEs can also occur in silicate minerals [49–51]. On the other hand, Sc^{3+} in a VI coordination has a radius of approximately 0.75 Å, similar to Mg^{2+} (VI coordination: 0.72 Å) and Fe^{2+} (VI coordination: 0.78 Å), allowing them to readily substitute for Mg, Fe^{2+}, Zr, and Sn within lattices [2]. It is worth noting that pure metallic forms of REEs are rarely found in nature; instead, they typically exist as compounds or isomorphisms within minerals [35,52]. The ionic radius of trivalent REE cations ranges from approximately 0.86 Å to 1.03 Å in VI coordination, similar to those of Na^{+}, Ca^{2+}, and Th^{4+} (VI coordination: 1.02 Å, 1.06 Å, and 1.15 Å, respectively) [13,49], which can enter minerals through isomorphism substitutions: Ca^{2+} + $(Nb, Ta)^{5+}$ ↔ REE^{3+} + Ti^{4+} (titanates, niobates, and tantalates), $2Ca^{2+}$ ↔ REE^{3+} + Na^{+} (perovskite), REE^{3+} + Si^{4+} ↔ Ca^{2+} + P^{5+} (apatite), Ca^{2+} + Th^{4+} ↔ $2REE^{3+}$ (apatite), Ca^{2+} + (Al, Fe^{3+}) ↔ REE^{3+} + Fe^{2+} (allanite), and Ca^{2+} + Si^{4+} ↔ REE^{3+} + (Al, Fe^{3+}) (garnet) [53–59].

HREEs are much less abundant than LREEs, primarily due to their lower concentration in Earth's crust [6,11,37,50,60]. Another contributing factor is that natural REE ores predominantly contain La, Ce, and Nd with a significantly lower proportion of HREEs [8,13]. The primary ore minerals for LREEs are monazite ((Ce, La, Nd, Th) PO_4) and bastnäsite ((Ce, La) (CO_3) F), while HREEs mainly originate from xenotime (YPO_4), apatite ($Ca_5(PO_4)_3$(F, Cl, OH)), eudialite ($(Na, Ca, Ce)_6(Zr, Fe)_2Si_7$(O, OH, $Cl)_{22}$), and ion adsorption clay deposits [6,9,12,61]. In addition to independent minerals, Sc often occurs in mafic minerals such as pyroxene and hornblende. Common Sc-containing minerals include thortveitite ($Sc_2Si_2O_7$), pretulite ($ScPO_4$), kolbeckite ($ScPO_4 \cdot 2H_2O$), jervisite ($NaScSi_2O_6$), and other minerals [62].

Nowadays, more than 270 different REE-bearing minerals have been identified [63], including bastnäsite, monazite, xenotime, allanite, pyrochlore, anatase, perovskite, ilmenite, rutile, and zircon (Table 2) [12,34,35,47,50,52,64–67]. As a result, silicate minerals account for approximately 43% of the total REE-bearing minerals, followed by carbonate minerals at 23%, oxide minerals at 14%, phosphate minerals at 14%, and other oxygen-containing salt minerals [9,11,47]. Except for xenotime, which is not influenced by crustal REE abundance, various REE-bearing minerals generally exhibit higher LREE contents compared to HREEs [68].

Table 2. REE-rich minerals and chemical formulas.

Mineral	Chemical Formula
Bastnäsite	(Ce, La, Nd, Y…) CO_3F
Parisite	Ce_2Ca $(CO_3)_3F_2$
Monazite	(Ce, La) PO_4
Xenotime	YPO_4
Fluocerite	(Ce, La) F_3
Eudialyte	$Na_4(Ca,Ce)_2(Fe^{2+},Mn^{2+},Y)ZrSi_8O_{22}(OH,Cl)_2$
Pyrochlore	$(Ca, Na, REE)_2Nb_2O_6(OH, F)$ [1]
Vitusite	$Na_3(Ce, La, Nd)$ $(PO_4)_2$ [1]
Fergusonite	Y (Nb, Ta) O_3
Perovskite	(Ca, REE) TiO_3 [1]
Ilmenite	$Y_2(SiO_4)$ (CO_3)
Gadolinite	$(Y, Ce)_2Fe^{2+}Be_2Si_2O_{10}$
Ancylite	Sr (Ce, La) $(CO_3)_2OH \cdot H_2O$ [1]
Apatite	$(Ca, REE, Sr, Na, K)_3Ca_2(PO_4)_3(F, OH)$

Table 2. *Cont.*

Mineral	Chemical Formula
Doverite	$YCaF(CO_3)_2$ [1]
Jervisite	$NaScSi_2O_6$
Kolbeckite	$ScPO_4 \cdot 2H_2O$
Pretulite	$ScPO_4$
Thortveitite	$Sc_2Si_2O_7$

[1] representative chemical formulas are provided here.

4. Types of REE Deposits

REE deposits can be classified into various categories based on their geological settings [8,10,50,69,70]. Recently, Goodenough et al. (2018) [8] divided REE ore deposits into two categories according to formation temperature [8]: (1) high-temperature REE deposits formed through magmatic and hydrothermal processes, commonly associated with carbonatite rocks, alkaline igneous rocks, and hydrothermal systems [63,71–80], where carbonatite-related REE deposits are the primary source of LREEs, accounting for approximately 51.4% of global rare earth oxide (REO) resources and 97% of China's rare earth resources [11,81]. The Bayan Obo and Maoniuping deposits in China are also the world's largest and third-largest rare earth deposits [30,82–85]; (2) low-temperature REE deposits formed by low-temperature processes, such as erosion and weathering. These include placer, bauxite, laterite, and ion adsorption clay deposits [8,11,12,50,63,86–90]. The ion adsorption clay deposits in South China are globally renowned for their significant contribution to the supply of HREEs [61,91–93].

Under the current REE supply system, LREEs primarily originate from REE deposits associated with carbonatite, while ion adsorption clay deposits in southern China are the dominant source of HREEs globally [60,94]. Carbonatites are igneous rocks composed of more than 50 vol% primary carbonate minerals such as calcite and dolomite [95] and exhibit the highest REE content among all igneous rocks [7,96]. The chondrite-normalized REE pattern in carbonatite demonstrates a remarkable enrichment of LREEs [7,78,97–99], which was likely achieved through (1) crystallization of primitive magma rich in REEs and (2) evolution of residual magma experiencing fluid activity in the late stage of magma [100–102]. The occurrence of abundant hydrothermal REE minerals (including barite, apatite, and fluorite, [81,88,103,104]) indicates significant hydrothermal activity in the Bayan Obo REE deposit. The hydrothermal processes are believed to play an important role during carbonatite REE mineralization [82,83,105]. Fluorine (F)- and phosphorus (P)-containing minerals like bastnäsite, xenotime, and monazite have also been discovered in other hydrothermal REE deposits [106,107]. The presence of these minerals indicates that F^-,SO_4^{2-}, and PO_4^{3-} in hydrothermal fluids play a crucial role in transporting and/or depositing REEs [67,108,109] during carbonatite-related REE mineralization.

The ion adsorption deposits in southern China have undergone a synergistic superposition of magmatism and weathering, which is well-documented. The granitic parent rocks, rich in REEs, underwent weathering, releasing REEs from minerals within the granites into the fluid phases. Subsequently, the REEs were adsorbed as ionic complexes by clay minerals present on the weathering crusts [61,89,110].

5. REE Complexes in Various Hydrothermal Fluids

Previous studies on natural samples from REE deposits, such as the Bayan Obo large REE deposit, the Dalucao breccia deposit, the Yinachang Fe–Cu-(REE) deposit, and the Sin Quden Iron Oxide–Copper–Gold (IOCG) deposit have provided evidence of fluid activities [30,32,33,83,98,107,111–118]. Zhang et al. (2022) [118] discovered high-density, CO_2-rich, low-salinity (<5 wt.% $NaCl_{equiv}$) fluid inclusions in fluorite of the Dalucao breccia deposit. The fluid inclusions contain a significant amount of SO_4^{2-} along with small amounts of chloride (3.1%) and carbonate (4.4%) species. Therefore, SO_4^{2-} is believed

to transport REEs during the magmatic–hydrothermal stage. Xie et al. (2015) [119] analyzed fluid inclusions from the Maoniuping deposit and found that they contained up to 20 wt.% S and less than 1 wt.% Cl. Li and Zhou (2015) [31] discovered that fluids with varying compositions exert diverse effects on the mobility of REEs through fluorapatite geochemistry in the Yinachang deposit [31]. Fluid inclusions contain H_2O, CO_2, alkali, and other ligands, including F^-, OH^-, Cl^-, SO_4^{2-}, CO_3^{2-}, and PO_4^{3-} [7,30,115,118].

Natural sample data, including fluid inclusions, have substantiated the presence of hydrothermal activity within REE deposits. Subsequent investigations have further confirmed the significant contribution of fluid activity in the transport and redistribution of REEs. Notably, in the Bayan Obo REE deposit, multiple phases of fluid activity have been identified, with fluids exerting a predominant influence on the redistribution and activation of REEs within minerals [116]. Similarly, in the Strange Lake REE–Zr deposit located in Canada, REEs were observed to transport alongside acidic fluids, with REE deposition and mineralization occurring as the fluid pH levels increased [120]. With advancing technology, an increasing number of studies such as in-situ XAS, Raman spectroscopy, and LA-ICP-MS on fluid inclusions have substantiated that fluid interaction plays a pivotal role in the genesis of REE deposits within carbonatite and alkaline igneous rocks [34,71,82,98,100,109,121–125]. The aforementioned research confirms that during magma evolution, hydrothermal fluids typically influence the activation and transport of REEs, while different aqueous ligands bind to REEs within melts or minerals, causing REE leaching from melt or mineral phases into fluids where they are transported as complexes [34,71,82,98,100,109,121–125]. These studies highlight the significant role of fluids in the activation, transport, and mineralization of REEs [87,126,127].

Turner et al. (1981) [128] investigated the hydrolysis behaviors of various elemental ions at pH = 8.2 and I = 0.65 (the value of ionic strength in mol/L), revealing that, except Sc, most REEs are resistant to hydrolysis at ambient temperature and can exist predominantly as ions in solution, while Sc exhibits partial hydrolysis [128] (Figure 2). Zero hydrolysis of most REE ions suggests that the predominant forms of REEs in solution are REE ions or hydrated ions in low-temperature and acidic to weakly basic fluids [34,61]. This could potentially serve as a crucial factor enabling REEs to form ion adsorption deposits.

Besides REE ions or hydrated ions, REEs can also exist as complexes, which could be dominated by the activity of ligands and the fluid's pH. Generally, with the ligand activity increasing, REE complexes prevail over hydrated ions. As pH increases, the hydrolysis of REEs intensifies, and REE–hydroxyl species dominate in solutions (Figure 3). Consequently, REE complexes might exert a significant influence on the transport of REEs during magmatic–hydrothermal processes.

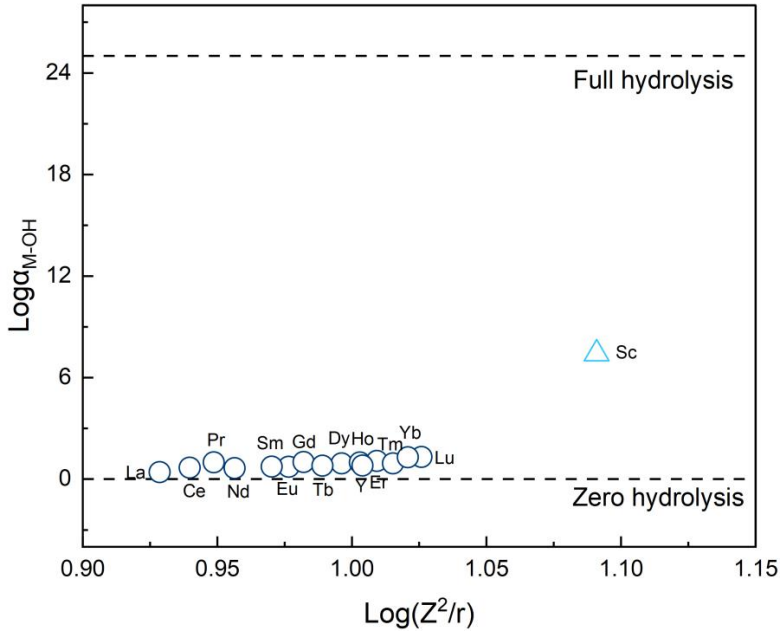

Figure 2. Plot of log$\alpha_{M\text{-}OH}$ vs. log(z^2/r) for REE cations (3+) at 25 °C, pH = 8.2, and I = 0.65 suggesting that most REE ions hardly hydrolyze until the fluid's pH reaches 8.2, whereas Sc ions display weak hydrolysis behavior. logαM-OH represents the hydrolysis degree of REE ions following the reaction: $REE^{3+} + 3H_2O = REE(OH)_3 + 3H^+$, which is collected from [128]. Log(z^2/r) stands for the strength degree of ionic polarization force, in which z is the valence state and r refers to the ionic radii [129]. Almost zero hydrolysis of most REE ions implies that REEs can exist in the form of REE ions or hydrated ions in low-temperature and acidic–weakly basic fluids.

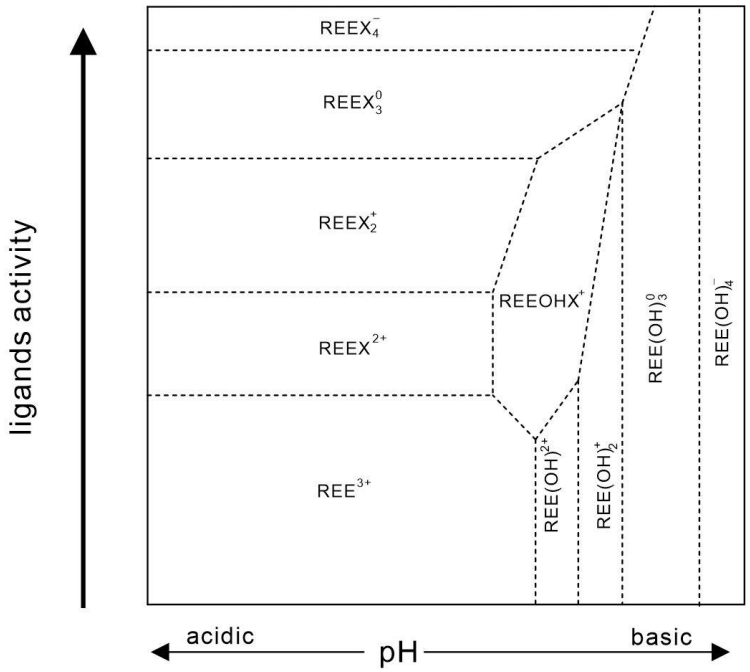

Figure 3. Model prediction illustrating the potential dominant species in fluids corresponding to the fluid's pH and the complexing ligand's activity based on the regular rules of ion complexation. X represents the ligand only, assuming its valence state is −1. Because REEs display zero and weak hydrolysis, the stability fields of REE ions in fluids could be larger than those of most ore-forming metal ions, while the formation of the complexes would benefit from high complexing ligand activity.

According to the theory of "soft–hard acids and bases" [130], REEs are classified as hard acids and are expected to selectively bind with basic ligands such as F^-, SO_4^{2-}, CO_3^{2-}, PO_4^{3-}-, and other hard base ligands [131]. Moreover, due to slight differences in atomic radii, the solubility of various REEs with the same ligands also varies [131–133]. Therefore, the stability of complex species significantly influences the presence of REEs in hydrothermal fluids.

High-temperature experiments conducted in the last century have postulated that REEs may predominantly exist as halogen complexes in hydrothermal solutions [134,135]. Theoretical predictions and thermodynamic experimental studies on REE-bearing solutions have confirmed that REEs can be transported and enriched in high-temperature fluids through complexation with ligands including F^-, Cl^-, PO_4^{3-}, SO_4^{2-}, CO_3^{2-}, and OH^- [34,54,108,109,131,133,136–141]. Among these ligands, Cl^-, F^-, and SO_4^{2-} have been further investigated for their roles in the transport and deposition of REEs [34,54,109,131,134–140,142–147]. Cl acts as a versatile base capable of forming diverse complexes with hard/soft acids, rendering REEs highly susceptible to the influence of high-salinity fluids [85,109]. Recent studies have shown that Na and K ions in fluids can also enhance the stability of REE complexes and enhance their transport capacity [99,148].

The research on the hydrothermal activity of REEs not only focuses on the species and stability of the complexes but also the solubility of REE-containing minerals [34,109,125,149]. However, due to the complex and diverse nature of these minerals, thermodynamic data has only been verified for a few fluorinated and phosphate minerals containing REEs (bastnasite, fluorite, xenotime) [34,68,109,131], while most other REE-containing minerals lack sufficient thermodynamic data.

5.1. REE Fluoride Complexes

Fluorite and F-containing carbonates, including bastnäsite and parisite, are commonly encountered in magmatic–hydrothermal REE deposits. IOCG deposits are also rich in REEs [106,112,150,151]. Considering the ability of F to form stable REE–F complexes [152–155], most studies suggest that the fluids associated with REE transport and mineralization primarily contain F. These studies explain the deposition mechanism of REEs in F-bearing fluids through three processes, namely, (1) the reaction between the mineralizing fluid and Ca-rich wall rock/fluid to generate low-solubility fluorite; (2) the defluorination of ore-forming fluid leading to a decrease in the activity of F in the fluid; and (3) the destruction of the stability of REE–F complexes [47,151,156,157].

Fluorine can decrease the solidus temperature and viscosity of silicate melts, as well as enhance ion diffusion rates [46,158–161]. Additionally, it can increase the solubility of minerals such as zircon, monazite, ilmenite, and rutile in fluids or melts [162–167]. This prevents REEs from being incorporated into these minerals and promotes their enrichment in residual melts [168]. However, recent findings by Duan et al. (2023) [169] suggest that F does not directly facilitate REE transport. Nevertheless, a high F content in magma could influence its crystallization history and result in REE enrichment followed by removal through exsolved volatiles.

Numerous studies have been conducted on the complexation and speciation of REEs in hydrothermal systems containing F [34,54,108,109,131,136,138,170–173], covering a temperature range from 5 °C to 500 °C. Based on the thermodynamic conclusions of [108], Luo and Miller (2004) [173] investigated the stability of $REEF^{2+}$ and $REEF_2^+$ complexes. Their results were consistent within the temperature range of 5~40 °C, with lower stability observed for LREE–F complexes compared to HREE–F complexes. Migdisov et al. (2009) [131] compared the first formation constants of REE–F and REE–Cl complexes based on their new experimental results [131] and discovered that at high temperatures, the stability of the LREE–F complex exceeded that of the HREE–F complex (Figure 4). They considered that the high-temperature data reported by [108] was extrapolated from ambient temperature rather than obtained through actual measurements at high temperatures. It is worth

noting that all these studies confirmed an increase in the stability of REE–F complexes as temperatures rise.

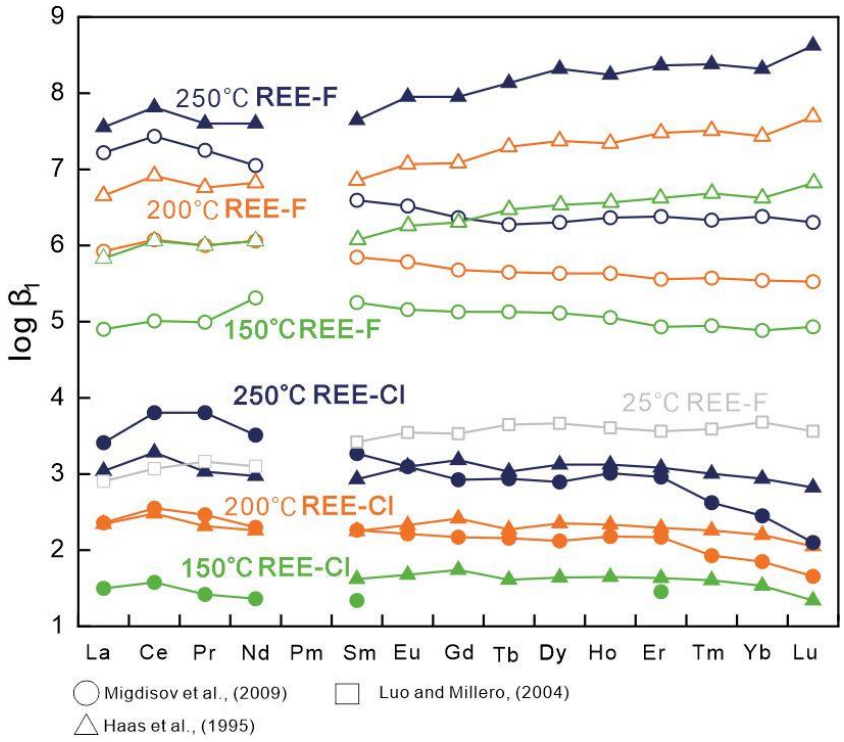

Figure 4. A comparison of the first formation constants of the complexes ($REE^{3+} + F^- = REEF^{2+}$; $REE^{3+} + Cl^- = REECl^{2+}$) shows that the stability of REE–F complexes is several orders of magnitude higher than that of REE–Cl complexes. The data are from [108,131,173].

In chloride–fluoride hydrothermal systems, Migdisov and Williams-Jones (2014) [109] discovered that, under acidic conditions, Nd primarily exists as $NdCl^{2+}$ and $NdCl_2^+$; however, as the solution becomes neutral, the dominant species shifts to Nd–F complexes, resulting in a significant decrease in Nd concentration in the solution (<1 ppb) due to the precipitation of NdF_3. On the other hand, under alkaline conditions, Nd predominately exists as $Nd(OH)_3^0$ and $Nd(OH)_2^+$. With increasing temperature, there is an intensified complexation of Nd with chloride and a gradual increase in the pH boundary for both Nd–chloride and Nd–fluoride from 3.5 at 200 °C to 4 at 300 °C and to 6.4 at 400 °C. It can be observed that low-temperature and neutral conditions are favorable for the formation of Nd–fluoride complexes. However, due to its low solubility in F-containing solutions, the transport of Nd by such solutions is limited. In addition, the complex forms of Ce (representing LREE) and Er (representing HREE) are similar to those of Nd under different conditions [109]. Although aqueous REE–fluoride complexes ($REEF^{2+}$ and $REEF_2^+$) exhibit remarkable stability at ambient temperature [131], thermodynamic models suggest that the solubility of these complexes is relatively low at higher pH levels. Furthermore, at lower pH levels, the solution activity of REE–fluoride complexes also decreases, resulting in hindrances and reduced efficiency in transporting REEs in F-containing hydrothermal at any stage. Hence, it is speculated that F is more likely to serve as the primary binding ligand for depositing REEs [109,133].

According to the above geochemical studies, it is proposed that REE–F complexes are not the primary form of REE transport. This belief stems from several key factors. Firstly, HF^0 usually displays weak ionization, resulting in a limited release of F^- ions for complexing metal anions [174,175]. During geological processes, hydrothermal fluids containing REE are typically acidic to neutral, which compresses the stability range of REE–F [34,117]. Similarly, Cl is widely present in hydrothermal settings as an anionic

ligand with an average content of 10 wt.% [109], while F is mostly present in ppm levels in solution, except for abnormal enrichment [72]. Moreover, high temperatures further inhibit its ionization process, such that F- only exists in abundance under neutral to weakly alkalic conditions [133,176]. Secondly, the favorable pH range for transporting REEs closely aligns with that required for $REEF_3$ precipitation, resulting in low levels of soluble REEs [109]. Lastly, the solubility product of $REEF_3$ is much lower than that of $REECl_3$ [109]. Consequently, as fluoride content increases, it may even decrease the concentration of dissolved REEs [138].

At present, research is scarce on Yttrium. Loges et al. (2013) [177] experimentally demonstrated that in aqueous solutions containing F, yttrium exhibits a higher degree of fluorination. At temperatures ranging from 100 to 250 °C with fluoride concentrations between 1 and 330 mmol/L, YF_2^+ predominates significantly over YF^{2+}.

5.2. REE Chloride Complex

In carbonatite and alkaline igneous REE deposits, Cl^- and SO_4^{2-} are commonly found as ligands in fluids [33,127]. Recent studies have confirmed the important role of chloride complexes in transporting REEs. Fluid inclusion data suggests that ore-forming fluids exhibit high salinity (32%~37% $NaCl_{eqv}$) and low pH, indicating that REEs may exist in the form of chloride complexes (Jbel Boho LREE vein, Morocco) [178]. Furthermore, chlorine has been identified as a primary ligand for transporting REEs based on studies conducted on the Dalucao brecciated ore REE deposit in China and the Sin Quye hydrothermal IOCG REE deposit in Vietnam, where it was observed to be present in numerous fluorite fluid inclusions [33,115]. Experimental studies on metal fluid/melt transport have also shown that the partition coefficient ($D_{fluid/melt}$) of REEs increases with chloride content in fluids [179]. Payne et al. (2023) [180] conducted fluorite solubility and REE transport experiments at different pHs, salinities, and temperatures. The experiments showed that adding NaCl can enhance the solubility of REEs in base solutions, with concentrations in the fluid reaching similar levels to the acidic solutions (i.e., NaCl-free and NaCl solutions). In the simulation study of complex species, it was also found that variations in pH and ligands lead to distinct dominant species of REE in the solution [34,180].

Louvel et al. (2015) employed XAS (X-ray absorption) to investigate the solubility of Yb and observed that under hydrothermal conditions with pH < 2 and $NaCl_{eqv}$ > 5 wt.%, the formation of aqueous REE complexes was favored, resulting in a significant increase in Yb solubility ($\approx n \times 1000$ ppm) [181]. Studies also indicate that chloride occurs predominantly as $REECl^{2+}$ and $REECl_2^+$ in fluids [34]. Migdisov and Williams-Jones (2014) [109] conducted experiments to analyze Nd complex species in solutions containing chloride, revealing that a NaCl solution with a concentration of 10 wt.% at various temperatures could transport 200 ppm of Nd within a high pH range (pH = ~ 5). The stability of REE–Cl complexes decreases with increasing atomic numbers at elevated temperatures (Figure 4). Therefore, LREEs, compared to HREEs, is more susceptible to being transported by Cl^-.

At low pH and high temperatures, HF exhibits weaker ionization compared to HCl and predominantly exists in the form of HF^0 in the fluid [47,174,175], while chlorine mostly exists as Cl^-. Thermodynamic simulation and hydrothermal experiments demonstrate that the stability of LREE–chloride complexes at high temperatures is higher than previously expected, whereas the stability of HREE–chloride complexes is overestimated (Figure 4) [34,108]. In comparison to the solubility of $REEF_3$, $REECl_3$ exhibits higher solubility, indicating a stronger ability for chloride to transport REEs. As a result, chlorine may serve as the primary ligand for REE transport and enrichment in hydrothermal fluids [34,176].

5.3. REE Sulfate Complex

Previous studies have demonstrated that SO_4^{2-} could serve as a ligand for the transport of REEs during the magmatic–hydrothermal process [85,127,181–186], and it has been identified in various deposits, such as the Yinachang Fe–Cu–(REE) deposit and Dalucao breccia deposit. A compositional analysis of hydrothermal fluids from the Mutnovsky

volcano in the Kamchatka area reveals that an increase in pH (pH < 6) leads to a decrease in REE concentration within hydrothermal systems. Particularly, acidic hydrothermal fluids containing SO_4^{2-} exhibit significantly higher ΣREE concentrations compared to alkaline hydrothermal fluids containing CO_3^{2-} [187], suggesting that SO_4^{2-} is more favorable to REE dissolution and transport compared to CO_3^{2-}. Similarly, in carbonatite systems, sulfate (SO_4^{2-}) proves to be more effective than Cl^- for transporting REEs due to its greater formation constant for REE-SO_4^{2-} complexes (Figures 4 and 5). Moreover, numerous species of polynuclear complex elements associated with REE-SO_4^{2-} complexes may possess stronger capabilities for transporting REEs [34,141,147,188,189]. Other experimental studies have also highlighted the significance of the REE-SO_4^{2-} complex in facilitating the transport of REEs under high-temperature conditions and weakly acidic to near-neutral pH levels [109,139]. Therefore, sulfate is widely recognized as a crucial complexing agent for facilitating the transport of REEs within hydrothermal systems [109,119].

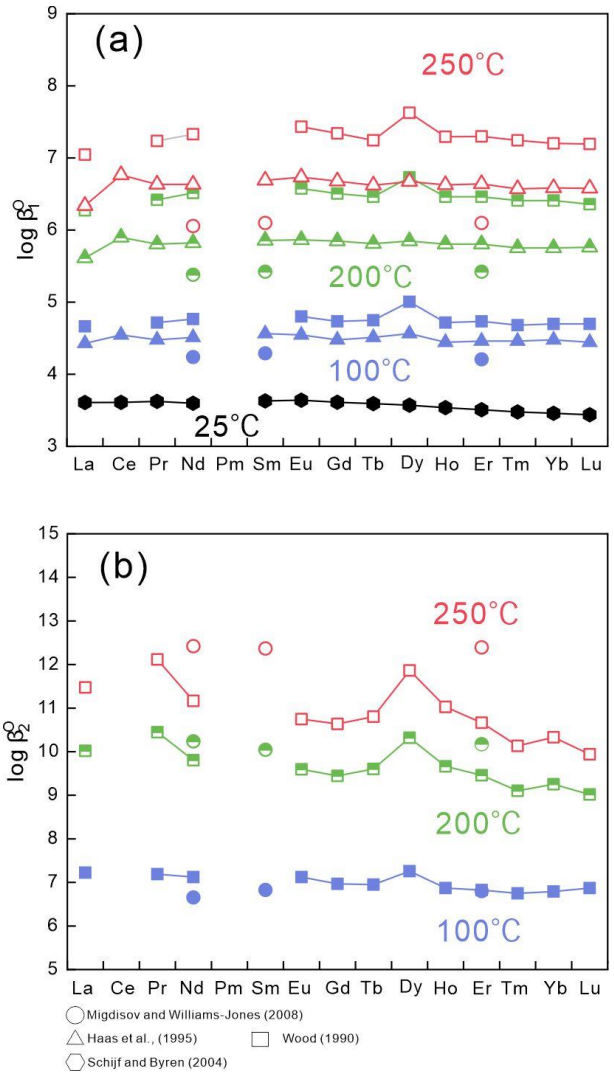

Figure 5. Comparison of the first (**a**) and second (**b**) formation constants of REE-SO_4^{2-} complexes suggesting that elevated temperature facilitates the formation of $REESO_4^+$ and $REE(SO_4)_2^-$ complexes and that the stability of $REE(SO_4)_2^-$ species is higher than that of $REESO_4^+$ at similar temperatures. The date from [54,108,139,190].

Determining the formation constants of $REESO_4^+$ and $REE(SO_4)_2^-$ complexes is important for comprehending the transport and enrichment of REEs in hydrothermal fluids

containing sulfates [54,136,139,190]. Previous studies have demonstrated that the stability of $REESO_4^+$ at high temperatures, as reported by [108] and [136], exceeds the calculated values provided by [139]. Although there was a minor discrepancy between these two datasets at ambient temperature, this difference becomes more pronounced with increasing temperatures (Figure 5). While not explicitly discussed by [139], previous research on chloride and fluoride complexes suggests that this phenomenon may be attributed to variations in HKF parameters (e.g., G: Gibbs free energy, α: activity). At ambient temperature, the stability of the $REESO_4^+$ complex slightly decreases with the atomic number [190]; however, this variation among elements is even smaller than the calculation uncertainty. Migdisov et al. (2016) [34] proposed that this insignificant difference has less impact on the stability of the $REESO_4^+$ complex at high temperatures since temperature escalation does not significantly alter its stability [34].

In high-temperature hydrothermal fluids, REEs mainly exist in the form of $REE(SO_4)_2^-$ complexes, while the abundance of mono-sulfate $REESO_4^+$ complexes is relatively low [109]. Experimental studies have indicated that REE-SO_4^{2-} complexes play a significant role in saturated aqueous solutions containing quartz due to REEs' close association with SO_4^{2-} ions [189], which can be attributed to the breakdown of SiO_2 at high temperatures facilitating sulfate dissolution and enhancing the binding between REEs and SO_4^{2-} ions. Rudolph and Irmer (2015) [191] confirmed the presence of $LaSO_4^+$ in a solution at 100 °C through in situ Raman observation, although $La(SO_4)_2^-$ was not detected. Wan observed diverse complex forms of REE-SO_4^{2-} at high temperatures including $REE(SO_4)_2^-$ and $REESO_4^+$, as well as REE-HSO_4^{2-} and other polynuclear complexes, inferring that the REE-HSO_4^{2-} and polynuclear complexes may play a more significant role in transporting REEs [147]. Furthermore, under high pressures and temperatures, there is a substantial increase in the solubility of REEs in sulfate-containing solutions [141].

Migdisov and Williams-Jones (2014) [109] conducted experiments on the complexation of Nd in a chloride–sulfate solution and determined that $Nd(OH)_3$ was the sole solid precipitate formed. The pH range of Nd transport in the solution is wide (400 °C, pH < 7.5), exceeding that observed in solutions containing only chloride (pH < 5). Furthermore, the prevalence of REE–Cl complexes is limited to low-pH acidic conditions (300 °C, pH < 2). Migdisov et al. (2016) [34] consider that the enhanced transport capability of SO_4^{2-} can be attributed to its approximately 2.5–3.5 orders of magnitude higher stability compared to REE–Cl complexes; however, there is currently no definitive explanation for the predominance of REE–Cl complexes under strongly acidic conditions. In summary, it can be confirmed that SO_4^{2-} can act as a transporting ligand for REEs.

5.4. REE Carbonate Complexes

Carbonates are considered to be a significant phase for incorporating REEs, and the ability of CO_3^{2-} to transport REEs has become a prominent research topic in recent years [30,32,76,79,83,192]. The enrichment of REEs and thorium in carbonatites is often associated with hydrothermal activity [71,82,100,122,193]. Under ambient conditions, carbonate complexes are highly stable [192,194,195]. Cantrell and Byrne (1987) [194] confirmed that $REECO_3^+$ and $REE(CO_3)_2^-$ are the primary aqueous complexes of REEs in seawater, with LREEs being preferentially associated with $REECO_3^+$ and HREEs preferentially associated with $REE(CO_3)_2^-$.

Previous thermodynamic predictions suggest that the stability of REE–carbonate complexes at temperatures up to 300 °C is comparable to those of REE–fluoride complexes [108,136]. However, Migdisov et al. (2016) [34] utilized extrapolated thermodynamic data on Eu–carbonate from previous studies and observed significant variations in values predicted by different researchers at different temperatures, indicating a serious lack of thermodynamic data for REE–CO_3^{2-} complexes [34]. By comparing the formation constants of REE–F complexes and REE–CO_3^{2-} complexes, it was found that the first formation constants for Eu–CO_3^{2-} complexes were higher than those for Eu–F complexes (Figures 4 and 6), indicating that the stability of REE–CO_3^{2-} complexes is greater than that of REE–F. Nonetheless, this data solely represents predicted

values under standard conditions, with discrepancies in high-temperature environments. Zhang et al. (2023) [85] discovered a large number of fluocerites from the Taipingzhen deposit during an early high-temperature hydrothermal stage. The study shows that earlier-formed fluocerites should be supplanted by later-formed bastnäsite. It was revealed that continuous exposure to high temperatures resulted in CO_2 release and the preservation of fluocerite, whereas, when temperature declined slowly, bastnaesite replaced fluocerite. Therefore, it can be predicted that the stability of REE–F complexes is greater than that of REE–CO_3^{2-} complexes at high temperatures.

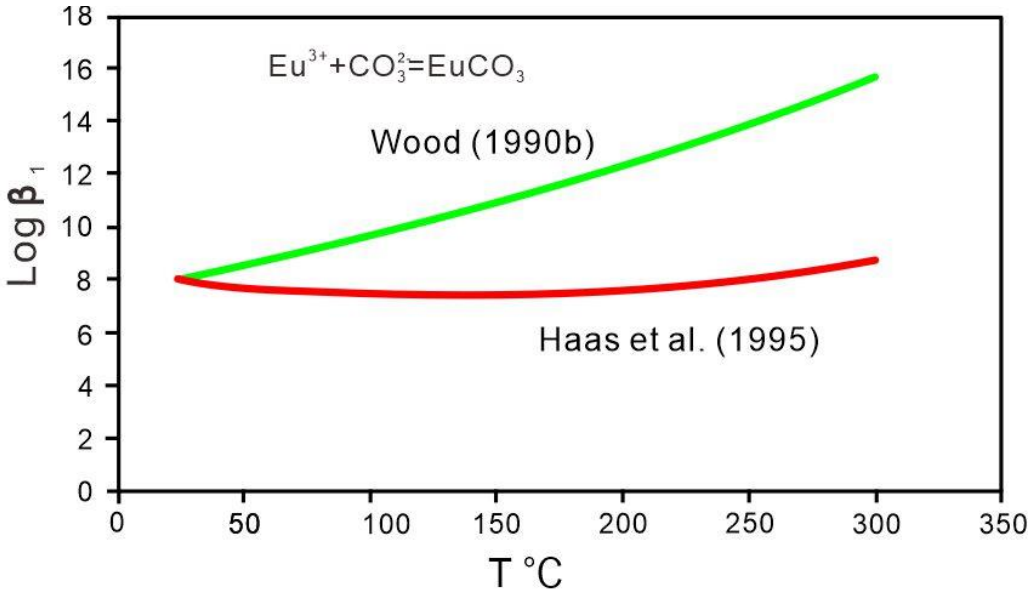

Figure 6. The values for the first formation constants of Eu–CO_3^{2-} [108,136].

In neutral fluids containing carbonate, REEs primarily exist in the form of carbonate complexes (HCO_3^- and/or CO_3^{2-}). However, under acidic conditions, the presence of carbonate complexes in solutions may be negligible, as mentioned by [196]. The high halogen content in hydrothermal systems could limit the formation of REE–CO_3^{2-} complexes. Other studies have suggested that in low-salinity fluids rich in CO_2, REEs can form complexes with CO_3^{2-}; in high salinity systems abundant in CO_2, REEs may be transported in the form of chlorine or sulfate complexes; and in alkaline fluids, REEs might occur in the form of REE–OH complexes [149]. Moreover, the solubilities of solid minerals corresponding to REE–CO_3^{2-} complexes are also low, suggesting that the effect of carbonate on transporting REEs in solutions may be minimal. However, recent research by [148] has shown that hydroxyl carbonate complexes can enhance the hydrothermal mobilization of REEs under alkaline conditions (LREE: >300 °C; HREE: <300 °C), which might be the main mechanism for redistributing REEs within carbonatite rocks [197]. The depletion of LREEs in hydrothermal fluids related to carbonatites in the Kamtai area may also be attributed to this mechanism. Moreover, fluid inclusion analysis of the Strange Lake (Canada) REE deposit reveals a pH variation for the ore-forming fluids, ranging from alkaline conditions (425 °C, pH ~ 10) to acidic conditions (300 °C, pH ~ 3) [124]. In alkaline solutions, HCO_3^- was considered a complexing agent for REEs due to charge balance considerations, abundant carbonic inclusions, and the presence of nahcolite. Additionally, based on experimental evidence [198], hydroxyl carbonate is also recognized as an important carrier of REEs, particularly in alkaline fluids. Fractional crystallization of carbonatite magma could lead to alkali enrichment in solutions [16,199–201], creating a favorable environment for the formation of alkaline hydrothermal fluids that potentially transport REEs through CO_3^{2-}.

5.5. REE Phosphate Complexes

Previous studies have suggested that the transport of REEs can be influenced by phosphate, and REEs may be transported in the form of phosphate complexes or in conjunction with other ligands. However, in hydrothermal systems rich in fluorine and phosphorus, it is challenging to extensively transport REEs [202], suggesting that phosphorus may play a similar role to F in transporting and depositing REEs. The remarkably low solubility of REE phosphate minerals (monazite and xenotime) also limits the amount of transferable REEs in fluids [75], making it unlikely for PO_4^{3-} to significantly impact REE transport [47]. Gysi studied the species of REE–phosphate/chlorine complexes and found that the content of soluble REEs in the H_3PO_4 system was minimal, whereas the total amount of soluble REEs in the HCl system was 2~4 orders of magnitude higher compared to the H_3PO_4 system when conducting experiments involving H_3PO_4–HCl–HF [203]. This suggests that the formation of REE–Cl complexes dominates REE transport, comparable to REE–F and REE–PO_4^{3-} complexes.

The experimental investigation of the REE–PO_4^{3-} complex further confirms that phosphate acts as the ligand for the deposition of REEs and has limited transport ability towards REEs. In natural hydrothermal systems with multiple ligands, REEs are often observed to be transported along with Cl^- or SO_4^{2-}, and subsequently precipitate with F^-, CO_3^{2-}, and PO_4^{3-}. However, the thermodynamic data regarding the REE–PO_4^{3-} complex and related minerals primarily rely on the theoretical predictions of [108], which also require additional thermodynamic data for supplementation.

5.6. REE Hydroxyl Complexes

REEs can also exist as hydroxyl complexes in hydrothermal solutions, such as $REE\left(OH\right)_3^0$, $REE\left(OH\right)_2^+$, and $REE\left(OH\right)^{2+}$ [204,205]. However, the only experimental study on the stability of REE–OH complexes to date was conducted by [142]. In comparison with theoretical calculations [108], the pH dominance range of Nd^{3+} at 290 °C is significantly broader. The contribution of $Nd(OH)^{2+}$ to the dissolution of Nd is slightly reduced, and the dominance range of $Nd(OH)_2^+$ is smaller than predicted, whereas under basic conditions, $Nd(OH)_3^0$ prevails more commonly [34] (Figure 7).

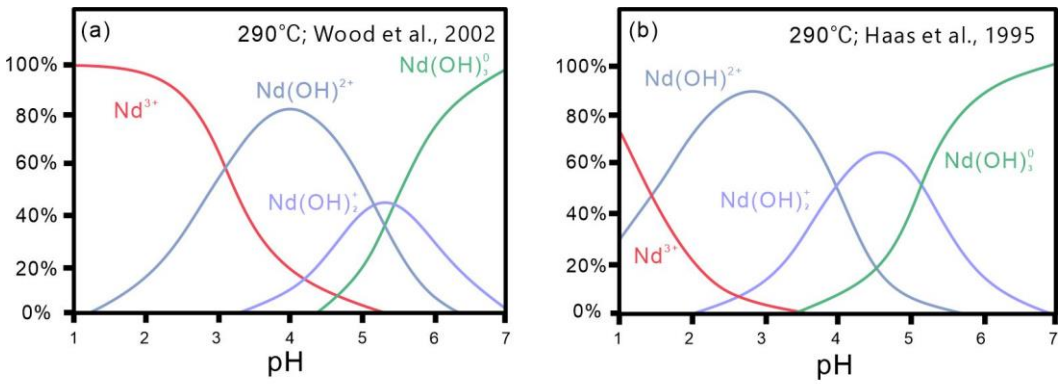

Figure 7. The relationship between dominant Nd species and pH is based on thermodynamic data at 290 °C [108,136]. Under acidic conditions (pH < 2), Nd mainly exists in the form of Nd^{3+} (**a**), while in neutral to base conditions (pH = 3~5), $Nd(OH)_2^+$ and $Nd(OH)_3^0$ are mainly dominated (**b**). Data from [108,142].

5.7. REE Organic Complexes

Lecumberri-Sanchez et al. (2018) [206] discovered a significant concentration of REEs in oil-bearing low-temperature basin brine ($\sum$REE > 1000 × *n* ppm) within the El Hammam Fluorite Mining Area, Morocco. They hypothesized that the enrichment of REEs in this region could be attributed to transportation facilitated by acetic acid complexes. Given

the diverse range of organic compounds present, investigating the stability of REE complexes associated with these compounds appears feasible. However, dealing with such complex systems poses a considerable challenge due to their distinct properties. Furthermore, organic compounds often exhibit property changes at high temperatures, further complicating research efforts.

6. Geological Implications

The requirement for achieving REE enrichment at the ore-forming level is that the parent magma must contain a sufficient amount of REEs and undergo further enrichment through magma evolution. This process is influenced by factors such as the oxidation state of the magma, differentiation during crystallization, and enrichment in alkali elements [207–211]. Carbonatite and alkaline magmas may contain various volatile components, including CO_2, H_2O, Cl, F, and S [7,78,97–99]. As crystallization progresses, these components, along with various incompatible elements, accumulate in residual magma. They can then fractionate into separate fluid phases. The presence of fluid inclusions and evidence of alkaline metasomatism provide clear indications for the separation of volatile fluid phases [30,83,115]. Depending on the composition and evolution of the magma, the main minerals containing REEs can either crystallize directly from the magma, such as bastnäsite in the Mountain Pass deposit, or REEs can exist as an incompatible element in residual magma and be carried and distributed into the fluid phase by the exsolution fluids. The exsolution of the fluid phase from the melt is influenced not only by the composition of the melt but also by changes in temperature and pressure [7]. In high-temperature and high-pressure fluids, due to the enhanced hydrolysis of REEs, the dominant species of REE could change from simple hydrated ions to REE–ligand complexes [34,212]. Therefore, in the high-temperature environment of magmatic systems, the most influential factors on the transport of REE are often various ligands. These ligands play a vital role in facilitating the distribution of REEs within both magmatic and hydrothermal systems.

In acidic–neutral hydrothermal systems, the transport of REEs is primarily controlled by SO_4^{2-} and Cl^- ions, while the presence of F^-, CO_3^{2-}, and PO_4^{3-} ions play a crucial role in the deposition of REEs [34,109,121,139,180,213]. In alkaline hydrothermal systems, REEs mainly exist in solutions as hydroxyl complexes [181]. Additionally, in neutral to alkaline solutions, the formation of hydroxyl carbonate complexes becomes increasingly significant for REE deposition [148,149,181,198,204].

To further investigate the disparity in the transportability of REEs by Cl and F, the ionization constants were utilized to calculate their respective ionization and transport quantities. Figure 8 illustrates that REE–F complexes exhibit lower transport ability compared to REE–Cl complexes. Consequently, it can be inferred that chloride ions (Cl^-) should also serve as the preferred ligand for transporting REEs.

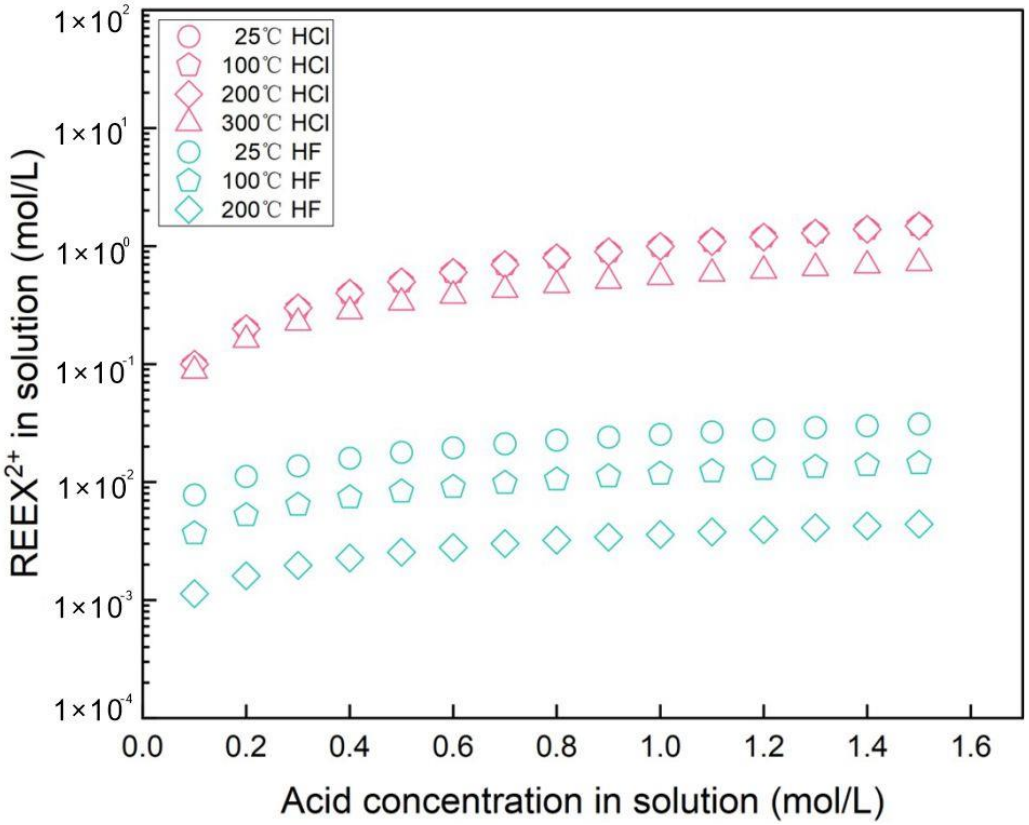

Figure 8. The model calculation reveals comparable transport capacity between the $REEF^{2+}$ complex and $REECl^{2+}$ complex based on the ionization equilibrium constant (K) of HCl and HF. Note that HCl is highly ionized below 200 °C. The $\log(K_{HF})$ used to calculate is −3.18 at 25 °C, −3.85 at 100 °C, and −4.89 at 200 °C [214], while $\log(K_{HCl})$ is 6.79 at 25 °C, 4.6 at 100 °C, 2.16 at 200 °C, and −0.18 at 300 °C [215].

As previously mentioned, the hydrolysis of REEs increases with rising temperature and pH levels. Consequently, at elevated temperatures, the transportation of REEs is predominantly governed by the presence of dominant complex species (Figures 2 and 3). However, as the temperature drops or pH decreases, REEs gradually exist in the solution primarily as REE^{3+} ions. Therefore, in low-temperature deposits, REE^{3+} ions are carried by fluids and subsequently absorbed by clay minerals within weathered clay zones. In hydrothermal deposits hosted in carbonatites and alkaline igneous rocks, REEs are transported as complexes and subsequently deposited as minerals. In geological processes, hydrothermal fluids often contain high concentrations of F^- ions [215] and/or other ligands [33,115,178]. Additionally, fluid inclusion analyses commonly reveal the presence of substances such as SO_4^{2-},CO_3^{2-}, and PO_4^{3-} ions [82,85,100,127,182–186,193,202]. Based on available data, the transport abilities of different ligands for REEs follow the order, at high temperature (T > 300 °C) and the same concentration (assuming the average content of chlorine of ~2.5 mol/L): $Cl^- \approx SO_4^{2-} > F^{--} \approx PO_4^{3-} > CO_3^{2-} > OH^-$ (under acidic conditions); $OH^- > SO_4^{2-} \approx Cl^- > F^-$ (under alkaline conditions) [34]. In this scenario, REE-CO_3^{2-}–OH complexes may exhibit greater transport abilities for REEs under alkaline conditions. It is important to note that this order applies only to strong acidic or strong alkaline conditions. The effects of temperature, pH, and ligand concentration on this order should not be overlooked, and specific circumstances require individual analysis.

7. Prospects for Future Research

There are still significant gaps in our understanding of the mechanisms governing the transport and enrichment of REEs in hydrothermal fluids. For instance, there remains a

lack of knowledge regarding the complex species formed by REEs under high temperature and pressure conditions. As shown in Figure 3, there could be diverse potential dominant species in fluids corresponding to the fluid's pH and the complexing ligand's activity in theory; however, only a few have been confirmed so far. Additionally, the formation constants for REE complexes are insufficiently characterized, as are the thermodynamic parameters associated with REE minerals. Furthermore, further investigation is needed to elucidate the relationship between K/Na ratios and REE complexes, as well as how ambient conditions influence these complexes.

The study by Migdisov and Williams-Jones (2014) [109] is also based on the experimental findings of Banks et al. (1994) [182]. Although the overall conditions in these studies are relatively ideal, practical scenarios may involve additional factors that could influence the presence of HF in solutions and the formation of REE–F complexes. In geological processes, ore-forming fluids with high HF contents are commonly encountered [72,216]. However, it is still necessary to supplement new experimental data to determine whether higher coordinated REE–F complexes exist under high temperature and pressure conditions and establish thermodynamic data for REE–F complexes at elevated temperatures.

The experimental studies on sulfate systems indicate that sulfate is a key ligand for transporting REEs in hydrothermal solutions, leading to the mobility of a significant amount of REEs. However, it remains unclear which complex species enable the most efficient transport for REEs. Moreover, research on the complex species at temperatures exceeding 400 °C has yet to be conducted. Conclusions regarding the formation constants of REE–sulfate complexes are based on the experimental data, which indicates that REE–SO_4^{2-} complexes remain stable at temperatures above 250 °C. Nevertheless, these findings may have limitations, and further research is necessary to gain deeper insights into the transport behavior of REEs in sulfate systems at high temperatures.

The transport capacity of REE–chloride complexes is not internally restricted, unlike systems containing fluorine. This suggests that Cl can effectively transport significant amounts of REEs under specific pH conditions in natural hydrothermal systems. Recent research on the transport of chlorine in REEs has demonstrated that REEs can be transported as chloride complexes ($NdCl^{2+}$ and $NdCl_2^+$) within hydrothermal systems [34]. The transport potential of Cl in transporting REEs is substantial, making it an essential ligand for REEs in hydrothermal processes. Therefore, future research should focus primarily on exploring variations in partitioning coefficients of REEs in chloride-containing hydrothermal fluids across different systems, temperatures, and pressures to understand factors contributing to the selective enrichment of REEs during magmatic–hydrothermal or fluid activity stages.

The aforementioned studies on REE–CO_3^{2-}/REE–PO_4^{3-} complexes are primarily based on early thermodynamic calculations, which possess significant limitations. Currently, there is a dearth of research data on the behavior of REEs in carbonate/phosphate systems, and the theoretical framework remains incomplete. Therefore, conducting thermodynamic investigations into REEs in carbonatites holds immense significance and practical value. The range of existence for REE–OH complexes is constrained due to insufficient thermodynamic data and limited research efforts that have only focused on a few elements, resulting in a scarcity of available reliable information.

In addition, further comprehensive investigations are still required, including into the significantly higher degree of fluorination observed in Y compared to other REEs [177] and the general absence of Sc combining with common mineralization anions. These distinctive elemental properties necessitate additional supplementation; moreover, there exists a wide range of organic ligands whose physicochemical characteristics undergo alterations under both high and low temperatures. Therefore, it is imperative to conduct extensive research on REE organic complexes.

8. Conclusions

Based on the geological observations on REE mobility and mineralization, as well as the published data on REE solubility, speciation in hydrothermal solutions, and related thermodynamic calculations, this paper reviewed and compared the complexation and REE transport capacity of various hydrothermal fluids. The major conclusions are as follows:

(1) Zero or weak hydrolysis of REE ions suggests that the predominant forms of REEs in solution are REE ions or hydrated ions in low-temperature and acidic–weakly basic fluids.

(2) Cl^-, SO_4^{2-}, and OH^- are the main ligands for transporting REEs, while F^-, CO_3^{2-}, and PO_4^{3-} are the ligands for depositing REEs. Organic matter may also be a complexing ligand for the transport of REEs.

(3) The REE transport abilities of different ligands with similar concentrations under high-temperature (T > 300 °C) acidic or alkaline conditions follow the order: $Cl^- \approx SO_4^{2-} > F^- \approx PO_4^{3-} > CO_3^{2-} > OH^-$ (acidic conditions); $OH^- > SO_4^{2-} \approx Cl^- > F^-$ (alkaline conditions). REE-CO_3^{2-}–OH complexes may exhibit greater transport abilities for REEs under alkaline conditions.

(4) The transport of REEs is affected by the ligand types and environmental factors such as temperature, pressure, pH, and the ligand activity in fluids. A scenario with high temperature, low pH, high ligand content, and high salinity will enhance the dissolution and transport of REEs in hydrothermal fluids.

Author Contributions: Conceptualization, X.D.; investigation, J.D.; writing—original draft preparation, J.D.; writing—review and editing, X.D.; funding acquisition, X.D. All authors have read and agreed to the published version of the manuscript.

Funding: This study was supported by funds from the Guangdong Major Project of Basic and Applied Basic Research (Grant NO. 2019B030302013), the Strategic Priority Research Program of the Chinese Academy of Sciences (XDB42000000). This is also contribution No. IS-3519 from GIGCAS.

Data Availability Statement: No new data were created or analyzed in this study. Data sharing is not applicable to this article.

Conflicts of Interest: The authors declare no conflicts of interest.

References

1. Gupta, C.K.; Krishnamurthy, N. Extractive metallurgy of rare earths. *Int. Mater. Rev.* **1992**, *37*, 197–248. [CrossRef]
2. Connelly, N.G.; Damhus, T.; Hartshorn, R.M.; Hutton, A.T. *Nomenclature of Inorganic Chemistry IUPAC Recommendations 2005*; The Royal Society of Chemistry: Cambridge, UK, 2005; p. 366. Available online: http://web.archive.org/web/20080527204340/http:/www.iupac.org/publications/books/rbook/Red_Book_2005.pdf (accessed on 1 July 2022).
3. Henderson, P. (Ed.) General geochemical properties and abundances of the rare earth elements. In *Rare Earth Elements Geochemistry*; Elsevier: Amsterdam, The Netherlands, 1984; pp. 1–32.
4. Wang, Z.G. *Geochemistry of Rare Earth Elements*; Science Press: Beijing, China, 1989; pp. 1–496. (In Chinese)
5. Brugger, J.; Lahaye, Y.; Costa, S.; Lambert, D.; Bateman, R. Inhomogeneous distribution of REE in scheelite and dynamics of Archaean hydrothermal systems (Mt. Charlotte and Drysdale gold deposits, Western Australia). *Contrib. Mineral. Petrol.* **2000**, *139*, 251–264. [CrossRef]
6. Hatch, G.P. Dynamics in the global market for rare earths. *Elements* **2012**, *8*, 341–346. [CrossRef]
7. Verplanck, P.L. The role of fluids in the formation of rare earth element deposits. *Procedia Earth Planet. Sci.* **2017**, *17*, 758–761. [CrossRef]
8. Goodenough, K.M.; Wall, F.; Merriman, D. The rare earth elements: Demand, global resources, and challenges for resourcing future generations. *Nat. Resour. Res.* **2018**, *27*, 201–216. [CrossRef]
9. Chakhmouradian, A.R.; Wall, F. Rare earth elements: Minerals, mines, magnets (and more). *Elements* **2012**, *8*, 333–340. [CrossRef]
10. Linnen, R.; Samson, I.M.; Williams-Jones, A.E.; Chakhmouradian, A.R. Geochemistry of the rare-earth element, Nb, Ta, Hf and Zr deposits. In *Treatise on Geochemistry*, 2nd ed.; Elsevier: Amsterdam, The Netherlands, 2014; Volume 13, pp. 543–568. [CrossRef]
11. Weng, Z.; Jowitt, S.M.; Mudd, G.M.; Haque, N. A detailed assessment of global rare earth element resources: Opportunities and challenges. *Econ. Geol.* **2015**, *110*, 1925–1952. [CrossRef]
12. Jha, M.K.; Kumari, A.; Panda, R.; Kumar, J.R.; Yoo, K.; Lee, J.Y. Review on hydrometallurgical recovery of rare earth metals. *Hydrometallurgy* **2016**, *165*, 2–26. [CrossRef]

13. Wall, F.; Rollat, A.; Pell, R.S. Responsible sourcing of critical metals. *Elements* **2017**, *13*, 313–318. [CrossRef]
14. Wall, F.; Pell, R. Responsible sourcing of rare earths: Exploration-stage intervention including life cycle assessment. In *Handbook on the Physics and Chemistry of Rare Earths*; Elsevier: Amsterdam, The Netherlands, 2020; Volume 58, pp. 155–194.
15. Chen, W.; Jiang, S.Y. How did carbonatite-related rare earth element deposits form? *Earth Sci.* **2022**, *47*, 3891–3893.
16. Song, W.; Xu, C.; Smith, M.P.; Kynicky, J.; Yang, J.; Liu, T.; Jing, D. Origin of heavy rare earth element enrichment in carbonatites. *Geochim. Cosmochim. Acta* **2023**, *362*, 115–126. [CrossRef]
17. Nassar, N.T.; Du, X.; Graedel, T.E. Criticality of the rare earth elements. *J. Ind. Ecol.* **2015**, *19*, 1044–1054. [CrossRef]
18. Balaram, V. Rare earth elements: A review of applications, occurrence, exploration, analysis, recycling, and environmental impact. *Geosci. Front.* **2019**, *10*, 1285–1303. [CrossRef]
19. European Commission. *Communication from the Commission to the European Parliament, the Council, the European Economic and Social Committee and the Committee of the Regions on the 2017 List of Critical Raw Materials for the EU*; Publications Office of the European Union: Brussels, Germany, 2017; 8p.
20. European Commission. Criticality Assessments, Deloitte Sustainability, British Geological Survey, Bureau de Recherches Géologiques et Minières, Netherlands Organisation for Applied Scientific Research. In *Study on the Review of the List of Critical Raw Materials*; Publications Office of the European Union: Brussels, Germany, 2017; 92p.
21. European Commission. Communication from the Commission to the European Parliament the Council, the European Economic and Social Committee and the Committee of the Regions. In *Critical Raw Materials Resilience: Charting a Path towards Greater Security and Sustainability*; Publications Office of the European Union: Brussels, Germany, 2020; 23p.
22. United States Geological Survey USGS. *Draft Critical Mineral List—Summary of Methodology and Background Information—U.S. Geological Survey Technical Input Document in Response to Secretarial Order No. 3359*; USGS: Reston, VA, USA, 2018; 15p.
23. Haxel, G. *Rare Earth Elements: Critical Resources for High Technology*; U.S. Department of the Interior, U.S. Geological Survey: Reston, VA, USA, 2002; Volume 87.
24. USDOE. *Critical Mineral Strategies*; U.S. Department of Energy: Washington, DC, USA, 2010; 165p.
25. Hoenderdaal, S.; Espinoza, L.T.; Marscheider-Weidemann, F.; Graus, W. Can a dysprosium shortage threaten green energy technologies? *Energy* **2013**, *49*, 344–355. [CrossRef]
26. Humphries, M. *Rare Earth Elements: The Global Supply Chain*; U.S. Congressional Research Service: Washington, DC, USA, 2013.
27. Ding, X.; Sun, W.D.; Chen, W.F.; Chen, P.R.; Sun, T.; Sun, S.J.; Lin, C.T.; Chen, F.K. Multiple Mesozoic magma processes formed the 240-185 Ma composite Weishan pluton, South China: Evidence from geochronology, geochemistry, and Sr-Nd isotopes. *Int. Geol. Rev.* **2015**, *57*, 1189–1217. [CrossRef]
28. Hoshino, M.; Sanematsu, K.; Watanabe, Y. REE mineralogy and resources. *Handb. Phys. Chem. Rare Earths* **2016**, *49*, 129–291. [CrossRef]
29. Wang, Y.; Hu, B.Q.; Wang, Q.; Li, Y.G.; Sun, Z.X.; Guo, G.L. Occurrence characteristic of HREE in Zoujiashan Uranium Deposit. *J. Jilin Univ. Erath Sci. Ed.* **2018**, *48*, 719–735.
30. Smith, M.P.; Henderson, P. Preliminary fluid inclusion constraints on fluid evolution in the Bayan Obo Fe-REE-Nb deposit, Inner Mongolia, China. *Econ. Geol.* **2000**, *95*, 1371–1388. [CrossRef]
31. Li, X.; Zhou, M.F. Multiple stages of hydrothermal REE remobilization recorded in fluorapatite in the Paleoproterozoic Yinachang Fe–Cu–(REE) deposit, Southwest China. *Geochim. Cosmochim. Acta* **2015**, *166*, 53–73. [CrossRef]
32. Fan, H.R.; Yang, K.F.; Hu, F.F.; Liu, S.; Wang, K.Y. The giant Bayan Obo REE-Nb-Fe deposit, China: Controversy and ore genesis. *Geosci. Front.* **2016**, *7*, 335–344. [CrossRef]
33. Li, X.C.; Zhou, M.F. The nature and origin of hydrothermal REE mineralization in the Sin Quyen deposit, northwestern Vietnam. *Econ. Geol.* **2018**, *113*, 645–673. [CrossRef]
34. Migdisov, A.; Williams-Jones, A.E.; Brugger, J.; Caporuscio, F.A. Hydrothermal transport, deposition, and fractionation of the REE: Experimental data and thermodynamic calculations. *Chem. Geol.* **2016**, *439*, 13–42. [CrossRef]
35. Jordens, A.; Cheng, Y.P.; Waters, K.E. A review of the beneficiation of rare earth element bearing minerals. *Miner. Eng.* **2013**, *41*, 97–114. [CrossRef]
36. Hedrick, J.B. *Minerals Yearbook: Volume I—Metals and Minerals*; USGS: Reston, VA, USA, 2000; p. 62.1.
37. Rudnick, R.L.; Gao, S. Composition of the continental crust. In *Treatise on Geochemistry*, 3rd ed.; Holland, H.D., Turekian, K.K., Eds.; Elsevier Pergamon: Oxford, UK, 2003; p. 56.
38. Weng, Z.H.; Jowitt, S.M.; Mudd, G.M.; Haque, N. Assessing rare earth element mineral deposit types and links to environmental impacts. *Appl. Earth Sci.* **2013**, *122*, 83–96. [CrossRef]
39. Sverjensky, D.A. Europium redox equilibria in aqueous solution. *Earth Planet. Sci. Lett.* **1984**, *67*, 70–78. [CrossRef]
40. Duan, Q.F. The Research of the Metallogenic Regularity of Stratabound Zinc-Lead Deposits from Sinian-Cambrian in the Western Hunan and Western Hubei. Ph.D. Thesis, University of Geosciences, Wuhan, China, 2014.
41. Sun, W.D.; Liang, H.Y.; Ling, M.X.; Zhan, M.Z.; Ding, X.; Zhang, H.; Yang, X.Y.; Li, Y.L.; Ireland, T.R.; Wei, Q.R.; et al. The link between reduced porphyry copper deposits and oxidized magmas. *Geochim. Cosmochim. Acta* **2013**, *103*, 263–275. [CrossRef]
42. Sun, W.D.; Huang, R.F.; Li, H.; Hu, Y.B.; Zhang, C.C.; Sun, S.J.; Zhang, L.P.; Ding, X.; Li, C.Y.; Zartman, R.E.; et al. Porphyry deposits and oxidized magmas. *Ore Geol. Rev.* **2015**, *65 Pt 1*, 97–131. [CrossRef]

43. Javanmard, S.R.; Tahmasbi, Z.; Ding, X.; Khalaji, A.A.; Hetherington, C.J. Geochemistry of garnet in pegmatites from the Boroujerd intrusive complex, Sanandaj-Sirjan zone, western Iran: Implications for the origin of pegmatite melts. *Mineral. Petrol.* **2018**, *112*, 837–856. [CrossRef]
44. Ding, X.; Lundstrom, C.; Huang, F.; Li, J.; Zhang, Z.M.; Sun, X.M.; Liang, J.L.; Sun, W.D. Nature and experimental constraints on formation of the continental crust based on niobium-tantalum fractionation. *Int. Geol. Rev.* **2009**, *51*, 473–501. [CrossRef]
45. Chang, A.F.; Ding, X. Thermodiffusion driven element and isotopic fractionations: A considerable component differentiation mechanism in silicate system. *Acta Petrol. Sin.* **2020**, *36*, 99–112.
46. Jiang, Z.H.; Ding, X.; Song, M.S.; Ling, M.X. Thermodiffusion of major and trace elements in dried aluminosilicate glass. *Ceram. Int.* **2022**, *48*, 28404–28412. [CrossRef]
47. She, H.D.; Fan, H.R.; Hu, F.F. Migration and precipitation of rare earth elements in the hydrothermal fluids. *Acta Petrol. Sin.* **2018**, *34*, 3567–3581.
48. Spedding, F.H. Contributions of the rare earths to science and technology. In *Symposium on the Effects of Rare Earths on the Properties of Metals and Alloys*; ASM: Cincinnati, OH, USA, 1975; pp. 1–11.
49. Mariano, A.N. Economic geology of rare earth elements. *Rev. Mineral. Geochem.* **1989**, *21*, 309–337.
50. Kanazawa, Y.; Kamitani, M. Rare earth minerals and resources in the world. *J. Alloys Compd.* **2006**, *408*, 1339–1343. [CrossRef]
51. Haque, N.; Hughes, A.; Lim, S.; Vernon, C. Rare earth elements: Overview of mining, mineralogy, uses, sustainability and environmental impact. *Resources* **2014**, *3*, 614–635. [CrossRef]
52. Kumari, A.; Panda, R.; Jha, M.K.; Kumar, J.R.; Lee, J.Y. Process development to recover rare earth metals from monazite mineral: A review. *Miner. Eng.* **2015**, *79*, 102–115. [CrossRef]
53. RØnsbo, J.G. Coupled substitutions involving REEs and Na and Si in apatites in alkaline rocks from the Ilimaussaq intrusion, South Greenland, and the petrological implications. *Am. Mineral.* **1989**, *74*, 896–901.
54. Wood, S.A. The aqueous geochemistry of the rare-earth elements and yttrium: 1. Review of available low-temperature data for inorganic complexes and the inorganic REE speciation of natural waters. *Chem. Geol.* **1990**, *82*, 159–186. [CrossRef]
55. Fleet, M.E.; Pan, Y. Site preference of rare earth elements in fluorapatite. *Am. Mineral.* **1995**, *80*, 329–335. [CrossRef]
56. Liang, T.; Wang, D.H.; Qu, W.J. REE geochemistry of calcites in the Dachang tin-polymetallic deposit, Guangxi. *Acta Petrol. Sin.* **2007**, *2310*, 2493–2503.
57. Tang, Y.Y.; Bi, X.W.; He, L.P. Geochemical characteristics of trace elements, fluid inclusions and carbon-oxygen isotopes of calcites in the Jinding Zn-Pb deposit, Lanping, China. *Acta Petrol. Sin.* **2011**, *279*, 2635–2645.
58. Hughes, J.M.; Rakovan, J.F. Structurally robust, chemically diverse: Apatite and apatite supergroup minerals. *Elements* **2015**, *11*, 165–170. [CrossRef]
59. Hu, Y.S.; Ye, L.; Wei, C. REE geochemistry of the hydrothermal calcites from the Huayuan orefield, in the western Hunan, China. *Acta Mineral. Sin.* **2020**, *40*, 441–449.
60. Simandl, G.J. Geology and market-dependent significance of rare earth element resources. *Miner. Depos.* **2014**, *49*, 889–904. [CrossRef]
61. Xu, C.; Kynický, J.; Smith, M.P.; Kopriva, A.; Brtnický, M.; Urubek, T.; Song, W. Origin of heavy rare earth mineralization in South China. *Nat. Commun.* **2017**, *8*, 14598. [CrossRef] [PubMed]
62. Williams-Jones, A.E.; Vasyukova, O.V. The Econ. Geol. of scandium, the runt of the rare earth element litter. *Econ. Geol.* **2018**, *113*, 973–988. [CrossRef]
63. Dostal, J. Rare metal deposits associated with alkaline/peralkaline igneous rocks. In *Rare Earth and Critical Elements in Ore Deposits*; Society of Economic Geologists: Littleton, CO, USA, 2016.
64. Anthony, J.W.; Bideaux, R.A.; Bladh, K.W. *Handbook of Mineralogy, Mineralogical Society of America*; Mineralogical Society of America: Chantilly, VA, USA, 2001.
65. Ding, X.; Hu, Y.H.; Zhang, H.; Li, C.Y.; Ling, M.X.; Sun, W.D. Major Nb/Ta fractionation recorded in garnet amphibolite facies metagabbro. *J. Geol.* **2013**, *121*, 255–274. [CrossRef]
66. Long, K.R.; Van Gosen, B.S.; Foley, N.K.; Cordier, D. *The Principal Rare Earth Elements Deposits of the United States—A Summary of Domestic Deposits and a Global Perspective—U.S. Geological Survey Scientific Investigations Report 2010–5220*; USGS: Reston, VA, USA, 2010; pp. 1–104.
67. Wang, J.; Li, L.; Santosh, M.; Yan, G.Y.; Shen, J.F.; Yuan, M.W.; Li, S.R. Multistage ore formation in the world's largest REE-Nb-Fe deposit of Bayan Obo, North China Craton: New insights and implications. *Ore Geol. Rev.* **2023**, *164*, 105817. [CrossRef]
68. Gysi, A.P.; Williams-Jones, A.E. The thermodynamic properties of bastnäsite-(Ce) and parisite-(Ce). *Chem. Geol.* **2015**, *392*, 87–101. [CrossRef]
69. Wall, F. Rare earth elements. In *Critical Metals Handbook*; John Wiley & Sons: Hoboken, NJ, USA, 2014; pp. 312–339.
70. Wei, C.W.; Xu, C.; Fu, W. Research advances in experimental petrology and geochemistry of rare earth elements in magmatic and hydrothermal systems. *Acta Petrol. Sin.* **2022**, *3802*, 455–471.
71. Cheng, Z.; Zhang, Z.; Aibai, A.; Kong, W.; Holtz, F. The role of magmatic and post-magmatic hydrothermal processes on rare-earth element mineralization: A study of the Bachu carbonatites from the Tarim Large Igneous Province, NW China. *Lithos* **2018**, *314*, 71–87. [CrossRef]
72. Ding, X.; Su, K.; Yan, H.; Liang, J.; Sun, W. Effect of F-rich fluids on the A-type magmatism and related metal mobilization: New insights from the Fogang-Nankunshan-Yajishan igneous rocks in southeast China. *J. Earth Sci.* **2022**, *33*, 591–608. [CrossRef]

73. Dostal, J. Rare earth element deposits of alkaline igneous rocks. *Resources* **2017**, *6*, 34. [CrossRef]
74. London, D. Rare-element granitic pegmatites. *Rev. Econ. Geol.* **2016**, *18*, 165–194. [CrossRef]
75. Sheard, E.R.; Williams-Jones, A.E.; Heiligmann, M.; Pederson, C.; Trueman, D.L. Controls on the concentration of zirconium, niobium, and the rare earth elements in the Thor Lake rare metal deposit, Northwest Territories, Canada. *Econ. Geol.* **2012**, *107*, 81–104. [CrossRef]
76. Simandl, G.J.; Paradis, S. Carbonatites: Related ore deposits, resources, footprint, and exploration methods. *Appl. Earth Sci.* **2018**, *127*, 123–152. [CrossRef]
77. Xie, Y.L.; Verplanck, P.L.; Hou, Z.; Zhong, R. Rare earth element deposits in China: A review and new understandings. In *Mineral Deposits of China*; Society of Economic Geologists: Littleton, CO, USA, 2019.
78. Anenburg, M.; Broom-Fendley, S.; Chen, W. Formation of rare earth deposits in carbonatites. *Elements* **2021**, *17*, 327–332. [CrossRef]
79. Zhang, Y.F.; Zhang, P.; Liu, J.J. New research process and prospecting of Chishan endogenetic light rare earth deposit in Weishan Country in Shandong Province. *Shandong Land Resour.* **2022**, *38*, 19–25, (In Chinese with English abstract).
80. Zhan, Y.X.; Li, X.C.; Wu, B.; Yang, K.F.; Fan, H.R.; Li, X.H. The occurrence and genesis of HREE-rich minerals from the giant Bayan Obo deposit, China. *Ore Geol. Rev.* **2023**, *157*, 105438. [CrossRef]
81. Feng, M.; Song, W.; Kynicky, J.; Smith, M.; Cox, C.; Kotlanova, M.; Wei, C. Primary rare earth element enrichment in carbonatites: Evidence from melt inclusions in Ulgii Khiid carbonatite, Mongolia. *Ore Geol. Rev.* **2020**, *117*, 103294. [CrossRef]
82. Ling, M.X.; Liu, Y.L.; Williams, I.S.; Teng, F.Z.; Yang, X.Y.; Ding, X.; Sun, W.D. Formation of the world's largest REE deposit through protracted fluxing of carbonatite by subduction-derived fluids. *Sci. Rep.* **2013**, *3*, 1776. [CrossRef]
83. Song, W.; Xu, C.; Smith, M.P.; Chakhmouradian, A.R.; Brenna, M.; Kynický, J.; Tang, H. Genesis of the world's largest rare earth element deposit, Bayan Obo, China: Protracted mineralization evolution over ~1 by. *Geology* **2018**, *46*, 323–326. [CrossRef]
84. Liu, Y.; Chakhmouradian, A.R.; Hou, Z.; Song, W.; Kynický, J. Development of REE mineralization in the giant Maoniuping deposit (Sichuan, China): Insights from mineralogy, fluid inclusions, and trace-element geochemistry. *Miner. Depos.* **2019**, *54*, 701–718. [CrossRef]
85. Zhang, W.; Chen, W.T.; Williams-Jones, A.E. An unique, fluocerite-rich REE deposit in Henan province, Central China: The missing link in magmatic-hydrothermal REE mineralizing systems? *Contrib. Mineral. Petrol.* **2023**, *178*, 34. [CrossRef]
86. Kynicky, J.; Smith, M.P.; Xu, C. Diversity of rare earth deposits: The key example of China. *Elements* **2012**, *8*, 361–367. [CrossRef]
87. Jaireth, S.; Hoatson, D.M.; Miezitis, Y. Geological setting and resources of the major rare-earth-element deposits in Australia. *Ore Geol. Rev.* **2014**, *62*, 72–128. [CrossRef]
88. Xie, Y.L.; Hou, Z.; Goldfarb, R.J.; Guo, X.; Wang, L. Rare earth element deposits in China. In *Rare Earth and Critical Elements in Ore Deposits*; Society of Economic Geologists: Littleton, CO, USA, 2016.
89. Borst, A.M.; Smith, M.P.; Finch, A.A.; Estrade, G.; Villanova-de-Benavent, C.; Nason, P.; Geraki, K. Adsorption of rare earth elements in regolith-hosted clay deposits. *Nat. Commun.* **2020**, *11*, 4386. [CrossRef]
90. Lohmeier, S.; Machleidt, J.; Klemd, R.; Ellmies, R. Okorusu tailings—Part II: REE mineralisation, and oxygen and carbon isotope variations. *S. Afr. J. Geol.* **2023**, *126*, 315–336. [CrossRef]
91. Li, J.; Peng, K.; Wang, P.; Zhang, N.; Feng, K.; Guan, D.; Yang, Q. Critical rare-earth elements mismatch global wind-power ambitions. *One Earth* **2020**, *3*, 116–125. [CrossRef]
92. Nassar, N.T.; Brainard, J.; Gulley, A.; Manley, R.; Matos, G.; Lederer, G.; Fortier, S.M. Evaluating the mineral commodity supply risk of the US manufacturing sector. *Sci. Adv.* **2020**, *6*, eaay8647. [CrossRef]
93. Xing, J.; Jiang, Y.; Xian, H.; Yang, W.; Yang, Y.; Tan, W.; Zhu, J. Hydrothermal alteration and the remobilization of rare earth elements during reprecipitation of nano-scale apatite in phosphorites. *Lithos* **2023**, *444*, 107113. [CrossRef]
94. Bao, Z.; Zhao, Z. Geochemistry of mineralization with exchangeable REY in the weathering crusts of granitic rocks in South China. *Ore Geol. Rev.* **2008**, *33*, 519–535. [CrossRef]
95. Le Maitre, R.W.; Streckeisen, A.; Zanettin, B.; Le Bas, M.J.; Bonin, B.; Bateman, P. (Eds.) *Igneous Rocks: A Classification and Glossary of terms: Recommendations of the International Union of Geological Sciences Subcommission on the Systematics of Igneous Rocks*; Cambridge University Press: Cambridge, UK, 2005.
96. Wall, F.; Mariano, A.N. Rare earth minerals in carbonatites: A discussion centered on the Kangankunde Carbonatite, Malawi. In *Rare Earth Minerals—Chemistry, Origin and Ore Deposits*; Jones, A.P., Wall, F., Williams, C.T., Eds.; The Mineralogical Society Series 7; Chapman and Hall: New York, NY, USA, 1996; pp. 193–225.
97. Prokopyev, I.R.; Borisenko, A.S.; Borovikov, A.A.; Pavlova, G.G. Origin of REE-rich ferrocarbonatites in southern Siberia (Russia): Implications based on melt and fluid inclusions. *Mineral. Petrol.* **2016**, *110*, 845–859. [CrossRef]
98. Walter, B.F.; Steele-MacInnis, M.; Giebel, R.J.; Marks, M.A.; Markl, G. Complex carbonate-sulfate brines in fluid inclusions from carbonatites: Estimating compositions in the system H_2O-Na-K-CO_3-SO_4-Cl. *Geochim. Cosmochim. Acta* **2020**, *277*, 224–242. [CrossRef]
99. Anenburg, M.; Mavrogenes, J.A.; Frigo, C.; Wall, F. Rare earth element mobility in and around carbonatites controlled by sodium, potassium, and silica. *Sci. Adv.* **2020**, *6*, eabb6570. [CrossRef]
100. Moore, M.; Chakhmouradian, A.R.; Mariano, A.N.; Sidhu, R. Evolution of rare-earth mineralization in the Bear Lodge carbonatite, Wyoming: Mineralogical and isotopic evidence. *Ore Geol. Rev.* **2015**, *64*, 499–521. [CrossRef]
101. Ruberti, E.; Enrich, G.E.; Gomes, C.B.; Comin-Chiaramonti, P. Hydrothermal REE fluorocarbonate mineralization at Barra do Itapirapua, a multiple stockwork carbonatite, Southern Brazil. *Can. Mineral.* **2008**, *46*, 901–914. [CrossRef]

102. Yang, K.F.; Fan, H.R.; Santosh, M.; Hu, F.F.; Wang, K.Y. Mesoproterozoic carbonatitic magmatism in the Bayan Obo deposit, Inner Mongolia, North China: Constraints for the mechanism of super accumulation of rare earth elements. *Ore Geol. Rev.* **2011**, *40*, 122–131. [CrossRef]
103. Niu, H.C.; Lin, C.X. The genesis of the Mianning REE deposit, Sichuan Province. *Miner. Depos.* **1994**, *13*, 345–353.
104. Bell, K.; Zaitsev, A.N.; Spratt, J.; Fröjdö, S.; Rukhlov, A.S. Elemental, lead and sulfur isotopic compositions of galena from Kola carbonatites, Russia–implications for melt and mantle evolution. *Mineral. Mag.* **2015**, *79*, 219–241. [CrossRef]
105. Wei, C.W.; Deng, M.; Xu, C.; Chakhmouradian, A.R.; Smith, M.P.; Kynicky, J.; Fu, B. Mineralization of the Bayan Obo rare earth element deposit by recrystallization and decarbonation. *Econ. Geol.* **2022**, *117*, 1327–1338. [CrossRef]
106. Oreskes, N.; Einaudi, M.T. Origin of rare earth element-enriched hematite breccias at the Olympic Dam Cu-U-Au-Ag deposit, Roxby Downs, South Australia. *Econ. Geol.* **1990**, *85*, 1–28. [CrossRef]
107. Williams, M.R.; Holwell, D.A.; Lilly, R.M.; Case, G.N.; McDonald, I. Mineralogical and fluid characteristics of the fluorite-rich Monakoff and E1 Cu–Au deposits, Cloncurry region, Queensland, Australia: Implications for regional F–Ba-rich IOCG mineralisation. *Ore Geol. Rev.* **2015**, *64*, 103–127. [CrossRef]
108. Haas, J.R.; Shock, E.L.; Sassani, D.C. Rare earth elements in hydrothermal systems: Estimates of standard partial molal thermodynamic properties of aqueous complexes of the rare earth elements at high pressures and temperatures. *Geochim. Cosmochim. Acta* **1995**, *59*, 4329–4350. [CrossRef]
109. Migdisov, A.A.; Williams-Jones, A.E. Hydrothermal transport and deposition of the rare earth elements by fluorine-bearing aqueous liquids. *Miner. Depos.* **2014**, *49*, 987–997. [CrossRef]
110. Li, M.Y.H.; Zhou, M.F.; Williams-Jones, A.E. The genesis of regolith-hosted heavy rare earth element deposits: Insights from the world-class Zudong deposit in Jiangxi Province, South China. *Econ. Geol.* **2019**, *114*, 541–568. [CrossRef]
111. Lehmann, B.; Nakai, S.I.; Höhndorf, A.; Brinckmann, J.; Dulski, P.; Hein, U.F.; Masuda, A. REE mineralization at Gakara, Burundi: Evidence for anomalous upper mantle in the western Rift Valley. *Geochim. Cosmochim. Acta* **1994**, *58*, 985–992. [CrossRef]
112. Williams-Jones, A.E.; Samson, I.M.; Olivo, G.R. The genesis of hydrothermal fluorite-REE deposits in the Gallinas Mountains, New Mexico. *Econ. Geol.* **2000**, *95*, 327–341. [CrossRef]
113. Gammons, C.H.; Wood, S.A.; Pedrozo, F.; Varekamp, J.C.; Nelson, B.J.; Shope, C.L.; Baffico, G. Hydrogeochemistry and rare earth element behavior in a volcanically acidified watershed in Patagonia, Argentina. *Chem. Geol.* **2005**, *222*, 249–267. [CrossRef]
114. Fan, H.R.; Hu, F.F.; Yang, K.F.; Wang, K.Y. Fluid unmixing/immiscibility as an ore-forming process in the giant REE–Nb–Fe deposit, Inner Mongolian, China: Evidence from fluid inclusions. *J. Geochem. Explor.* **2006**, *89*, 104–107. [CrossRef]
115. Liu, Y.; Chen, Z.; Yang, Z.; Sun, X.; Zhu, Z.; Zhang, Q. Mineralogical and geochemical studies of brecciated ores in the Dalucao REE deposit, Sichuan Province, southwestern China. *Ore Geol. Rev.* **2015**, *70*, 613–636. [CrossRef]
116. Smith, M.P.; Campbell, L.S.; Kynicky, J. A review of the genesis of the world class Bayan Obo Fe–REE–Nb deposits, Inner Mongolia, China: Multistage processes and outstanding questions. *Ore Geol. Rev.* **2015**, *64*, 459–476. [CrossRef]
117. Gysi, A.P.; Williams-Jones, A.E.; Collins, P. Lithogeochemical vectors for hydrothermal processes in the Strange Lake peralkaline granitic REE-Zr-Nb deposit. *Econ. Geol.* **2016**, *111*, 1241–1276. [CrossRef]
118. Zhang, W.; Chen, W.T.; Mernagh, T.P.; Zhou, L. Quantifying the nature of ore-forming fluids in the Dalucao carbonatite-related REE deposit, Southwest China: Implication for the transport and deposition of REEs. *Miner. Depos.* **2022**, *57*, 935–953. [CrossRef]
119. Xie, Y.; Li, Y.; Hou, Z.; Cooke, D.R.; Danyushevsky, L.; Dominy, S.C.; Yin, S. A model for carbonatite hosted REE mineralisation—The Mianning–Dechang REE belt, Western Sichuan Province, China. *Ore Geol. Rev.* **2015**, *70*, 595–612. [CrossRef]
120. Gysi, A.P.; Williams-Jones, A.E. Hydrothermal mobilization of pegmatite-hosted REE and Zr at Strange Lake, Canada: A reaction path model. *Geochim. Cosmochim. Acta* **2013**, *122*, 324–352. [CrossRef]
121. Williams-Jones, A.E.; Palmer, D.A.S. The evolution of aqueous–carbonic fluids in the Amba Dongar carbonatite, India: Implications for fenitisation. *Chem. Geol.* **2002**, *185*, 283–301. [CrossRef]
122. Rankin, A.H.; Linnen, R.L.; Samson, I.M. Carbonatite-associated rare metal deposits: Composition and evolution of ore-forming fluids–the fluid inclusion evidence. *Rare-Elem. Geochem. Miner. Depos.* **2005**, *17*, 299–314.
123. Trofanenko, J.; Williams-Jones, A.E.; Simandl, G.J.; Migdisov, A.A. The nature and origin of the REE mineralization in the Wicheeda Carbonatite, British Columbia, Canada. *Econ. Geol.* **2016**, *111*, 199–223. [CrossRef]
124. Johannes Giebel, R.; Gauert, C.D.; Marks, M.A.; Costin, G.; Markl, G. Multi-stage formation of REE minerals in the Palabora Carbonatite Complex, South Africa. *Am. Mineral.* **2017**, *102*, 1218–1233. [CrossRef]
125. Vasyukova, O.V.; Williams-Jones, A.E. Direct measurement of metal concentrations in fluid inclusions, a tale of hydrothermal alteration and REE ore formation from Strange Lake, Canada. *Chem. Geol.* **2018**, *483*, 385–396. [CrossRef]
126. Ling, Q.C.; Liu, C.Q. Geochemical Behaviors of REE and Other Trace Elements during the Formation of Strata-bound Skarns and Related Deposits: A Case Study of the Dongguashan Cu (Au) Deposit, Anhui Province, China. *Acta Geol. Sin.* **2003**, *77*, 246–257.
127. Richter, L.; Diamond, L.W.; Atanasova, P.; Banks, D.A.; Gutzmer, J. Hydrothermal formation of heavy rare earth element (HREE)–xenotime deposits at 100 °C in a sedimentary basin. *Geology* **2018**, *46*, 263–266. [CrossRef]
128. Turner, D.R.; Whitfield, M.; Dickson, A.G. The equilibrium speciation of dissolved components in freshwater and sea water at 25 °C and 1 atm pressure. *Geochim. Cosmochim. Acta* **1981**, *45*, 855–881. [CrossRef]
129. Shannon, R.T.; Prewitt, C.T. Effective ionic radii in oxides and fluorides. *Acta Crystallogr. Sect. B Struct. Crystallogr. Cryst. Chem.* **1969**, *25*, 925–946. [CrossRef]
130. Pearson, R.G. Hard and soft acids and bases. *J. Am. Chem. Soc.* **1963**, *85*, 3533–3539. [CrossRef]

131. Migdisov, A.A.; Williams-Jones, A.E.; Wagner, T. An experimental study of the solubility and speciation of the Rare Earth Elements (III) in fluoride-and chloride-bearing aqueous solutions at temperatures up to 300 °C. *Geochim. Cosmochim. Acta* **2009**, *73*, 7087–7109. [CrossRef]
132. Bau, M. Rare-earth element mobility during hydrothermal and metamorphic fluid-rock interaction and the significance of the oxidation state of europium. *Chem. Geol.* **1991**, *93*, 219–230. [CrossRef]
133. Williams-Jones, A.E.; Migdisov, A.A.; Samson, I.M. Hydrothermal mobilisation of the rare earth elements–a tale of "ceria" and "yttria". *Elements* **2012**, *8*, 355–360. [CrossRef]
134. Williams-Jones, A.E.; Wood, S.A. A preliminary petrogenetic grid for REE fluorocarbonates and associated minerals. *Geochim. Cosmochim. Acta* **1992**, *56*, 725–738. [CrossRef]
135. Gammons, C.H.; Wood, S.A.; Williams-Jones, A.E. The aqueous geochemistry of the rare earth elements and yttrium: VI. Stability of neodymium chloride complexes from 25 to 300 °C. *Geochim. Cosmochim. Acta* **1996**, *60*, 4615–4630. [CrossRef]
136. Wood, S.A. The aqueous geochemistry of the rare-earth elements and yttrium: 2. Theoretical predictions of speciation in hydrothermal solutions to 350 °C at saturation water vapor pressure. *Chem. Geol.* **1990**, *88*, 99–125. [CrossRef]
137. Gammons, C.H. Complexation of the rare earth elements with aqueous chloride at 200° and 300 °C and saturated water vapor pressure. In *Water-Rock Interaction, Ore Deposits, Environmental Geochemistry*; The Geochemical Society: St. Louis, MO, USA, 2002; pp. 191–207.
138. Migdisov, A.A.; Williams-Jones, A.E. An experimental study of the solubility and speciation of neodymium (III) fluoride in F-bearing aqueous solutions. *Geochim. Cosmochim. Acta* **2007**, *71*, 3056–3069. [CrossRef]
139. Migdisov, A.A.; Williams-Jones, A.E. A spectrophotometric study of Nd III, Sm III and Er III complexation in sulfate-bearing solutions at elevated temperatures. *Geochim. Cosmochim. Acta* **2008**, *7221*, 5291–5303. [CrossRef]
140. Migdisov, A.; Guo, X.; Nisbet, H.; Xu, H.; Williams-Jones, A.E. Fractionation of REE, U, and Th in natural ore-forming hydrothermal systems: Thermodynamic modeling. *J. Chem. Thermodyn.* **2019**, *128*, 305–319. [CrossRef]
141. Wan, Y.; Chou, I.M.; Wang, X.; Wang, R.; Li, X. Hydrothermal sulfate surges promote rare earth element transport and mineralization. *Geology* **2023**, *51*, 449–453. [CrossRef]
142. Wood, S.A.; Palmer, D.A.; Wesolowski, D.J. The aqueous geochemistry of the rare earth elements and yttrium. Part XI. The solubility of Nd OH_3 and hydrolysis of Nd^{3+} from 30 to 290 °C at saturated water vapor pressure with in-situ pHm measurement. In *Water–Rock Interactions, Ore Deposits, and Environmental Geochemistry: A Tribute to David Crerar*; Special Publication; The Geochemical Society: St. Louis, MO, USA, 2002; Volume 7, pp. 229–256.
143. Mayanovic, R.A.; Jayanetti, S.; Anderson, A.J.; Bassett, W.A.; Chou, I.M. The structure of Yb^{3+} aquo ion and chloro complexes in aqueous solutions at up to 500 °C and 270 MPa. *J. Phys. Chem. A* **2002**, *106*, 6591–6599. [CrossRef]
144. Mayanovic, R.A.; Anderson, A.J.; Bassett, W.A.; Chou, I.M. On the formation and structure of rare-earth element complexes in aqueous solutions under hydrothermal conditions with new data on gadolinium aqua and chloro complexes. *Chem. Geol.* **2007**, *239*, 266–283. [CrossRef]
145. Mayanovic, R.A.; Anderson, A.J.; Bassett, W.A.; Chou, I.M. Steric hindrance and the enhanced stability of light rare-earth elements in hydrothermal fluids. *Am. Mineral.* **2009**, *94*, 1487–1490. [CrossRef]
146. Mayanovic, R.A.; Anderson, A.J.; Bassett, W.A.; Chou, I.M. The structure and stability of aqueous rare-earth elements in hydrothermal fluids: New results on neodymium (III) aqua and chloroaqua complexes in aqueous solutions to 500 °C and 520 MPa. *Chem. Geol.* **2009**, *259*, 30–38. [CrossRef]
147. Wan, Y.; Wang, X.; Chou, I.M.; Li, X. Role of sulfate in the transport and enrichment of REE in hydrothermal systems. *Earth Planet. Sci. Lett.* **2021**, *569*, 117068. [CrossRef]
148. Louvel, M.; Etschmann, B.; Guan, Q.; Testemale, D.; Brugger, J. Carbonate complexation enhances hydrothermal transport of rare earth elements in alkaline fluids. *Nat. Commun.* **2022**, *13*, 1456. [CrossRef]
149. Perry, E.P.; Gysi, A.P. Rare earth elements in mineral deposits: Speciation in hydrothermal fluids and partitioning in calcite. *Geofluids* **2018**, *2018*, 5382480. [CrossRef]
150. Huang, S.H.; Zhang, Z.M.; He, Y. Experimental geochemistry of rare earth elements. *Geol. Geochem.* **1986**, *11*, 29–33.
151. Deng, X.H.; Chen, Y.J.; Yao, J.M.; Bagas, L.; Tang, H.S. Fluorite REE-Y (REY) geochemistry of the ca. 850 Ma Tumen molybdenite–fluorite deposit, eastern Qinling, China: Constraints on ore genesis. *Ore Geol. Rev.* **2014**, *63*, 532–543. [CrossRef]
152. Bau, M.; Dulski, P. Comparative study of yttrium and rare-earth element behaviours in fluorine-rich hydrothermal fluids. *Contrib. Mineral. Petrol.* **1995**, *119*, 213–223. [CrossRef]
153. Pan, Y.; Fleet, M.E. Rare earth element mobility during prograde granulite facies metamorphism: Significance of fluorine. *Contrib. Mineral. Petrol.* **1996**, *1233*, 251–262. [CrossRef]
154. Petrella, L.; Williams-Jones, A.E.; Goutier, J.; Walsh, J. The nature and origin of the rare earth element mineralization in the Misery syenitic intrusion, northern Quebec, Canada. *Econ. Geol.* **2014**, *109*, 1643–1666. [CrossRef]
155. Estrade, G.; Salvi, S.; Béziat, D.; Williams-Jones, A.E. The origin of skarn-hosted rare-metal mineralization in the Ambohimirahavavy alkaline complex, Madagascar. *Econ. Geol.* **2015**, *110*, 1485–1513. [CrossRef]
156. Salvi, S.; Williams-Jones, A.E. The role of hydrothermal processes in concentrating high-field strength elements in the Strange Lake peralkaline complex, northeastern Canada. *Geochim. Cosmochim. Acta* **1996**, *60*, 1917–1932. [CrossRef]
157. Xu, C.; Kynicky, J.; Chakhmouradian, A.R.; Campbell, I.H.; Allen, C.M. Trace-element modeling of the magmatic evolution of rare-earth-rich carbonatite from the Miaoya deposit, Central China. *Lithos* **2010**, *118*, 145–155. [CrossRef]

158. Manning, D.A.C. The effect of fluorine on liquidus phase relationships in the system Qz-Ab-Or with excess water at 1 kb. *Contrib. Mineral. Petrol.* **1981**, *76*, 206–215. [CrossRef]
159. Dingwell, D.B.; Scarfe, C.M.; Cronin, D.J. The effect of fluorine on viscosities in the system Na_2O–Al_2O_3–SiO_2: Implications for phonolites, trachytes and rhyolites. *Am. Mineral.* **1985**, *70*, 80–87.
160. Giordano, D.; Romano, C.; Dingwell, D.B.; Poe, B.; Behrens, H. The combined effects of water and fluorine on the viscosity of silicic magmas. *Geochim. Cosmochim. Acta* **2004**, *68*, 5159–5168. [CrossRef]
161. Chen, C.; Ding, X.; Li, R.; Zhang, W.Q.; Ouyang, D.J.; Yang, L.; Sun, W.D. Crystal fractionation of granitic magma during its non-transport processes: A physics-based perspective. *Sci. China Earth Sci.* **2018**, *61*, 190–204. [CrossRef]
162. Rapp, J.F.; Klemme, S.; Butler, I.B.; Harley, S.L. Extremely high solubility of rutile in chloride and fluoride-bearing metamorphic fluids: An experimental investigation. *Geology* **2010**, *38*, 323–326. [CrossRef]
163. He, J.J.; Ding, X.; Wang, Y.R.; Sun, W.D.; Fu, B. The effect of temperature and concentration on hydrolysis of Fluorine-rich titanium complexes in hydrothermal fluids: Constraints on titanium mobility in deep geological processes. *Acta Petrol. Sin.* **2015**, *31*, 802–810.
164. Shao, T.B.; Xia, Y.; Ding, X.; Cai, Y.F.; Song, M.S. Zircon saturation model in silicate melts: A review and update. *Acta Geochim.* **2020**, *39*, 387–403. [CrossRef]
165. Di, J.; Yan, H.B.; Liu, Z.Y.; Ding, X. Synthesis and characterization of anatase TiO_2 microspheres self-assembled by ultrathin nanosheets. *Materials* **2021**, *14*, 2870. [CrossRef]
166. Yan, H.B.; He, J.J.; Liu, X.W.; Wang, H.B.; Liu, J.F.; Ding, X. Thermodynamic investigation of the hydrolysis behavior of fluorozirconate complexes at 423.15–773.15 K and 100 MPa. *J. Solut. Chem.* **2020**, *49*, 836–848. [CrossRef]
167. Yan, H.B.; Di, J.; Li, J.H.; Liu, Z.Y.; Liu, J.F.; Ding, X. Synthesis of Zirconia Micro-Nanoflakes with Highly Exposed (001) Facets and Their Crystal Growth. *Crystals* **2021**, *11*, 871. [CrossRef]
168. Keppler, H.; Wyllie, P.J. Partitioning of Cu, Sn, Mo, W, U, and Th between melt and aqueous fluid in the systems haplogranite-H_2O^- HCl and haplogranite-H_2O^- HF. *Contrib. Mineral. Petrol.* **1991**, *109*, 139–150. [CrossRef]
169. Duan, D.; Jiang, S.Y. Significant mobilization of REE from calc-alkaline melt into fluid during fluid exsolution: Insights from magmatic amphibole composition from Tieshan skarn Fe-Cu deposit (Hubei Province, China). *Ore Geol. Rev.* **2023**, *163*, 105759. [CrossRef]
170. Schijf, J.; Byrne, R.H. Determination of stability constants for the mono-and difluoro-complexes of Y and the REE, using a cation-exchange resin and ICP-MS. *Polyhedron* **1999**, *18*, 2839–2844. [CrossRef]
171. Luo, Y.R.; Byrne, R.H. The ionic strength dependence of rare earth and yttrium fluoride complexation at 25 °C. *J. Solut. Chem.* **2000**, *29*, 1089–1099. [CrossRef]
172. Luo, Y.R.; Byrne, R.H. The Influence of Ionic Strength on Yttrium and Rare Earth Element Complexation by Fluoride Ions in $NaClO_4$, $NaNO_3$ and NaCl Solutions at 25 °C. *J. Solut. Chem.* **2007**, *36*, 673–689. [CrossRef]
173. Luo, Y.; Millero, F.J. Effects of temperature and ionic strength on the stabilities of the first and second fluoride complexes of yttrium and the rare earth elements. *Geochim. Cosmochim. Acta* **2004**, *68*, 4301–4308. [CrossRef]
174. Hefter, G.T. Acidity constant of hydrofluoric acid. *J. Solut. Chem.* **1984**, *13*, 457–470. [CrossRef]
175. Ryzhenko, B.N.; Kovalenko, N.I.; Korsakova, N.V.; Mironenko, M.V. Ionization-Constant of Hydrofluoric-Acid at 500-Degrees-C, 1-KBAR. *Dokl. Akad. Nauk SSSR* **1991**, *317*, 203–206.
176. Liu, Y.; Chen, C.; Shu, X.C. The formation model of the carbonatite-syenite complex REE deposits in the east of Tibetan Plateau: A case study of Dalucao REE deposit. *Acta Petrol. Sin.* **2017**, *337*, 1978–2000.
177. Loges, A.; Migdisov, A.A.; Wagner, T.; Williams-Jones, A.E.; Markl, G. An experimental study of the aqueous solubility and speciation of Y (III) fluoride at temperatures up to 250 °C. *Geochim. Cosmochim. Acta* **2013**, *123*, 403–415. [CrossRef]
178. Benaouda, R.; Devey, C.W.; Badra, L.; Ennaciri, A. Light rare-earth element mineralization in hydrothermal veins related to the Jbel Boho alkaline igneous complex, AntiAtlas/Morocco: The role of fluid-carbonate interactions in the deposition of synchysite-(Ce). *J. Geochem. Explor.* **2017**, *177*, 28–44. [CrossRef]
179. Pokrovski, G.S.; Borisova, A.Y.; Bychkov, A.Y. Speciation and transport of metals and metalloids in geological vapors. *Rev. Mineral. Geochem.* **2013**, *76*, 165–218. [CrossRef]
180. Payne, M.R.; Gysi, A.P.; Hurtig, N.C. Hydrothermal fluorite solubility experiments and mobility of REE in acidic to alkaline solutions from 100 to 250 °C. *Chem. Geol.* **2023**, *617*, 121256. [CrossRef]
181. Louvel, M.; Bordage, A.; Testemale, D.; Zhou, L.; Mavrogenes, J. Hydrothermal controls on the genesis of REE deposits: Insights from an in situ XAS study of Yb solubility and speciation in high temperature fluids (T < 400 °C). *Chem. Geol.* **2015**, *417*, 228–237. [CrossRef]
182. Banks, D.A.; Yardley, B.W.D.; Campbell, A.R.; Jarvis, K.E. REE composition of an aqueous magmatic fluid: A fluid inclusion study from the Capitan Pluton, New Mexico, USA. *Chem. Geol.* **1994**, *113*, 259–272. [CrossRef]
183. Xie, Y.; Hou, Z.; Yin, S.; Dominy, S.C.; Xu, J.; Tian, S.; Xu, W. Continuous carbonatitic melt–fluid evolution of a REE mineralization system: Evidence from inclusions in the Maoniuping REE Deposit, Western Sichuan, China. *Ore Geol. Rev.* **2009**, *36*, 90–105. [CrossRef]
184. Lai, X.; Yang, X. Geochemical characteristics of the Bayan Obo giant REE–Nb–Fe deposit: Constraints on its genesis. *J. S. Am. Earth Sci.* **2013**, *41*, 99–112. [CrossRef]

185. Verplanck, P.L.; Hitzman, M. *Rare Earth and Critical Elements in Ore Deposits*; Reviews in Economic Geology; Society of Economic Geologists: Littleton, CO, USA, 2016; Volume 18. [CrossRef]
186. Giovannini, A.L.; Mitchell, R.H.; Neto, A.C.B.; Moura, C.A.; Pereira, V.P.; Porto, C.G. Mineralogy and geochemistry of the Morro dos Seis Lagos siderite carbonatite, Amazonas, Brazil. *Lithos* **2020**, *360*, 105433. [CrossRef]
187. Chudaev, O.V.; Chelnokov, G.A.; Bragin, I.V.; Kharitonova, N.A.; Rychagov, S.N.; Nuzhdaev, A.A.; Nuzhdaev, I.A. Rare earth and major elements geochemistry of geothermal waters from Mutnovsky volcano, Kamchatka. *Procedia Earth Planet. Sci.* **2017**, *17*, 92–95. [CrossRef]
188. Migdisov, A.A.; Williams-Jones, A.E. A spectrophotometric study of erbium (III) speciation in chloride solutions at elevated temperatures. *Chem. Geol.* **2006**, *234*, 17–27. [CrossRef]
189. Cui, H.; Zhong, R.; Xie, Y.; Yuan, X.; Liu, W.; Brugger, J.; Yu, C. Forming sulfate-and REE-rich fluids in the presence of quartz. *Geology* **2020**, *48*, 145–148. [CrossRef]
190. Schijf, J.; Byrne, R.H. Determination of SO4β1 for yttrium and the rare earth elements at I = 0.66 m and t = 25 °C—Implications for YREE solution speciation in sulfate-rich waters. *Geochim. Cosmochim. Acta* **2004**, *68*, 2825–2837. [CrossRef]
191. Rudolph, W.W.; Irmer, G.A. Raman spectroscopic investigation of speciation in $La_2(SO_4)_3$(aq). *RSC Adv.* **2015**, *5*, 84999–85008. [CrossRef]
192. Elliott, H.A.L.; Wall, F.; Chakhmouradian, A.R.; Siegfried, P.R.; Dahlgren, S.; Weatherley, S.; Deady, E. Fenites associated with carbonatite complexes: A review. *Ore Geol. Rev.* **2018**, *93*, 38–59. [CrossRef]
193. Walter, B.F.; Giebel, R.J.; Steele-MacInnis, M.; Marks, M.A.; Kolb, J.; Markl, G. Fluids associated with carbonatitic magmatism: A critical review and implications for carbonatite magma ascent. *Earth-Sci. Rev.* **2021**, *215*, 103509. [CrossRef]
194. Cantrell, K.J.; Byrne, R.H. Rare earth element complexation by carbonate and oxalate ions. *Geochim. Cosmochim. Acta* **1987**, *51*, 597–605. [CrossRef]
195. Johannesson, K.H.; Stetzenbach, K.J.; Hodge, V.F. Speciation of the rare earth element neodymium in groundwaters of the Nevada Test Site and Yucca Mountain and implications for actinide solubility. *Appl. Geochem.* **1995**, *10*, 565–572. [CrossRef]
196. Inguaggiato, C.; Censi, P.; Zuddas, P.; Londoño, J.M.; Chacón, Z.; Alzate, D.; D'alessandro, W. Geochemistry of REE, Zr and Hf in a wide range of pH and water composition: The Nevado del Ruiz volcano-hydrothermal system (Colombia). *Chem. Geol.* **2015**, *417*, 125–133. [CrossRef]
197. Patel, A.K.; Upadhyay, D.; Mishra, B.; Pruseth, K.L. Reconstruction of hydrothermal fluid composition of the Kamthai carbonatite complex, India using lattice strain model: Implications for LREE/HREE fractionation. *Lithos* **2023**, *444*, 107097. [CrossRef]
198. Nisbet, H.; Migdisov, A.A.; Goncharov, V.; van Hinsberg, V.; Williams-Jones, A.E.; Xu, H.; Guo, X. The solubility and speciation of Nd in carbonate-bearing hydrothermal fluids up to 250 °C. *Chem. Geol.* **2022**, *611*, 121122. [CrossRef]
199. Guzmics, T.; Mitchell, R.H.; Szabó, C.; Berkesi, M.; Milke, R.; Abart, R. Carbonatite melt inclusions in coexisting magnetite, apatite and monticellite in Kerimasi calciocarbonatite, Tanzania: Melt evolution and petrogenesis. *Contrib. Mineral. Petrol.* **2011**, *161*, 177–196. [CrossRef]
200. Weidendorfer, D.; Schmidt, M.W.; Mattsson, H.B. A common origin of carbonatite magmas. *Geology* **2017**, *45*, 507–510. [CrossRef]
201. Chayka, I.F.; Kamenetsky, V.S.; Vladykin, N.V.; Kontonikas-Charos, A.; Prokopyev, I.R.; Stepanov, S.Y.; Krasheninnikov, S.P. Origin of alkali-rich volcanic and alkali-poor intrusive carbonatites from a common parental magma. *Sci. Rep.* **2021**, *11*, 17627. [CrossRef] [PubMed]
202. Anenburg, M.; Mavrogenes, J.A. Carbonatitic versus hydrothermal origin for fluorapatite REE-Th deposits: Experimental study of REE transport and crustal "antiskarn" metasomatism. *Am. J. Sci.* **2018**, *318*, 335–366. [CrossRef]
203. Gysi, A.P.; Williams-Jones, A.E.; Harlov, D. The solubility of xenotime-(Y) and other HREE phosphates ($DyPO_4$, $ErPO_4$ and $YbPO_4$) in aqueous solutions from 100 to 250 °C and psat. *Chem. Geol.* **2015**, *401*, 83–95. [CrossRef]
204. Pourtier, E.; Devidal, J.L.; Gibert, F. Solubility measurements of synthetic neodymium monazite as a function of temperature at 2 kbars, and aqueous neodymium speciation in equilibrium with monazite. *Geochim. Cosmochim. Acta* **2010**, *74*, 1872–1891. [CrossRef]
205. Song, W.; Xu, C.; Veksler, I.V.; Kynicky, J. Experimental study of REE, Ba, Sr, Mo and W partitioning between carbonatitic melt and aqueous fluid with implications for rare metal mineralization. *Contrib. Mineral. Petrol.* **2016**, *171*, 1–12. [CrossRef]
206. Lecumberri-Sanchez, P.; Bouabdellah, M.; Zemri, O. Transport of rare earth elements by hydrocarbon-bearing brines: Implications for ore deposition and the use of REEs as fluid source tracers. *Chem. Geol.* **2018**, *479*, 204–215. [CrossRef]
207. Twyman, J.D.; Gittins, J. *Alkalic Carbonatite Magmas: Parental or Derivative? Special Publications*; Geological Society: London, UK, 1987; Volume 30, pp. 85–94. [CrossRef]
208. Chakhmouradian, A.R.; Zaitsev, A.N. Rare earth mineralization in igneous rocks: Sources and processes. *Elements* **2012**, *8*, 347–353. [CrossRef]
209. Watanabe, Y.; Kon, Y.; Echigo, T.; Kamei, A. Differential fractionation of rare earth elements in oxidized and reduced granitic rocks: Implication for heavy rare earth enriched ion adsorption mineralization. *Resour. Geol.* **2017**, *67*, 35–52. [CrossRef]
210. Bernard, C.; Estrade, G.; Salvi, S.; Béziat, D.; Smith, M. Alkali pyroxenes and amphiboles: A window on rare earth elements and other high field strength elements behavior through the magmatic-hydrothermal transition of peralkaline granitic systems. *Contrib. Mineral. Petrol.* **2020**, *175*, 1–27. [CrossRef]
211. Verplanck, P.L.; Mariano, A.N.; Mariano, A. Rare earth element ore geology of carbonatites. In *Rare Earth and Critical Elements in Ore Deposits*; Society of Economic Geologists: Littleton, CO, USA, 2016. [CrossRef]

212. Brugger, J.; Liu, W.; Etschmann, B.; Mei, Y.; Sherman, D.M.; Testemale, D. A review of the coordination chemistry of hydrothermal systems, or do coordination changes make ore deposits? *Chem. Geol.* **2016**, *447*, 219–253. [CrossRef]
213. Gysi, A.P.; Harlov, D.; Miron, G.D. The solubility of monazite ($CePO_4$), $SmPO_4$, and $GdPO_4$ in aqueous solutions from 100 to 250 °C. *Geochim. Cosmochim. Acta* **2018**, *242*, 143–164. [CrossRef]
214. Ellis, A.J. The effect of temperature on the ionization of hydrofluoric acid. *J. Chem. Soc.* **1963**, *823*, 4300–4304. [CrossRef]
215. Mei, Y.; Sherman, D.M.; Liu, W.; Etschmann, B.; Testemale, D.; Brugger, J. Zinc complexation in chloride-rich hydrothermal fluids (25–600 °C): A thermodynamic model derived from ab initio molecular dynamics. *Geochim. Cosmochim. Acta* **2015**, *150*, 265–284. [CrossRef]
216. Yan, H.B.; Ding, X.; Ling, M.X.; Li, C.Y.; Harlov, D.; Sun, W.D. Three late-Mesozoic fluorite deposit belts in southeast China and links to subduction of the (paleo)-Pacific plate. *Ore Geol. Rev.* **2021**, *129*, 103865. [CrossRef]

Disclaimer/Publisher's Note: The statements, opinions and data contained in all publications are solely those of the individual author(s) and contributor(s) and not of MDPI and/or the editor(s). MDPI and/or the editor(s) disclaim responsibility for any injury to people or property resulting from any ideas, methods, instructions or products referred to in the content.